2014

Modeling Repair Patches of Ship Hull and Studying the Effect of Their Orientation on Stresses

Halima Enwegy
University of Central Florida

MODELING REPAIR PATCHES OF SHIP HULL AND STUDYING THE EFFECT OF THEIR ORIENTATION ON STRESSES

by

HALIMA MOHAMED ENWEGY
MSME. University of Central Florida, 2013

A thesis submitted in partial fulfillment of the requirements
for the degree of Master of Science
in the Department of Mechanical Engineering
in the College of Engineering and Computer Science
at the University of Central Florida
Orlando, Florida

Spring Term
2014

Major Professor: Faissal A. Moslehy

ABSTRACT

The hull is the most important structural part of any maritime vessel. It must be adequately designed to withstand the harsh sailing environmental conditions and associated forces. In the past, the basic material used to manufacture the ship hull was wood, where the hull was usually shaped as cylindrical wooden shanks. In the present, hull designs have developed to steel columns or stiffened panels that are made of different types of materials. Panels that are stiffened orthogonally in two or more directions and have nine independent material constants are defined as orthotropic panels, and they achieve high specific strength.

This thesis presents the effect of different patch orientations on the resulting strain and stress concentrations at the area of interaction between the panel and the patch. As it is known, the behavior of stiffened plates is affected by several important parameters, e.g., length to width ratio of the panel, stiffener geometry and spacing, aspect ratio for plates between stiffeners, plate slenderness, von Mises stresses, initial distortions, boundary conditions, and type of loading. A finite element model of the ship hull has been developed and run on ABAQUS (commercially available finite element software). The stiffened panel and patch are modeled as equivalent orthotropic plates made of steel. The panel edges are considered to be simply supported, and uniaxial tension was applied to the equivalent stiffened panel in addition to the lateral pressure (from water interaction). The developed model successfully predicted the optimal orientation of the panel for maximum stress concentration reduction. Moreover, in order to minimize the severe conditions caused by the mismatch that occurs if the material properties of the patch and

the panel are the same during the patching process, it is necessary to stiffened the patch more than the panel. The developed model also suggested that an isotropic layer be added at the interaction to decrease the severity of arising stresses.

ACKNOWLEDGMENTS

I would never have been able to finish my thesis without the guidance of my committee members and the help and support of the kind people around me: my husband, family, and friends.

I would like to express the deepest appreciation to my committee chair Professor Faissal Moslehy, who has shown the attitude and substance of a genius: he continually and persuasively conveyed a spirit of adventure in regard to my research, and an excitement in regard to teaching. Without his supervision and constant guidance, this thesis would not have been possible.

I also had the pleasure of working with Professor David Nicholson for the past year. He introduced the idea of this research and was always willing to help. Although he is not present with us today, the work he did in giving me the opportunity to commence my academic progress is being presented today and will continue to exist in my life and career forever.

I would like to thank my committee members, Professor Yuanli Bai, for his excellent suggestions, beneficial criticism, and for allowing me to use his proprietary finite element code ABAQUS for my research. I would like to convey my sincere thanks to Professor Alain Kassab, who was a resource of information and helped me in my academic study.

In addition, I would like to thank my husband, Salem for his confidence, encouragement, and support, and my little boy, Suphyan for understanding why Mom could not always be there. You were always there cheering me up and stood by me during the good times and bad. You two are my light and the wind beneath my wings. I love you.

Finally, I would also like to thank my beloved parents. Words cannot express how thankful I am to my mother and father for all of the sacrifices that they have made on my behalf.

Your prayers for me are what have sustained me so far. Also, my thanks extend to my dear sisters and brothers who always supported and encouraged me with kind wishes and prayers. My lovely family, I owe you more than I can express.

TABLE OF CONTENTS

LIST OF FIGURES

LIST OF TABLES

CHAPTER 1: INTRODUCTION

In ship-building industries, the hull is the part of any maritime vessel that requires the most consideration, and careful selection of materials bearing specific properties is crucial to meet the intended structural performance. Additionally, it affects the ship's cost and strength.Therefore, it should be designed in such a way that allows it to withstand harsh environmental and weather conditions and reduces the effects of different forces and loads that act on the ship while sailing. Hull design depends on the type of the ship in which it is intended for use; in other words, naval architects use different methods of hull construction, keeping in mind the purpose and type of ship.

In the past, the basic material used to manufacture ships' hulls was wood, wherein the hull was usually formed with cylindrical wooden shanks. Nowadays, however, hull designs have developed to include steel columns or stiffened panels that are made of different types of materials. Panels that are stiffened orthogonally in two or more directions and have nine independent variables are defined as orthotropic panels. Such materials have recently been used in the ship-building industrybecause of their high specific strength. Moreover, the selection of the shape and material of stiffeners is essential in ship-building indusries in order to achieve designs at a minimal weight without sacrificing strength.

As the hull is in constant contact with water, it is subjected to different types of forces acting simultaneously. Subsequently, selection of materials is very important in hull structure design because it affects ship strength, durability, and increases resistance, which prevents structural damage in cases of collision or running aground. In hull structure design, the applied

force, the structural response calculations, and the secured responses are the three main categories that must be considered to achieve hull safety and reliability.

The hull consists of an outside covering and an inside framework to which the skin is secured. The main structural part of the hull is the keel, which runs from the stem at the bow (the front of the ship) to the sternpost at the stern (the rear of the ship). The keel is the backbone of the ship and gives shape and strength to the hull. Deck beams and bulkheads are other parts of the hull that support the decks and give additional strength to resist water pressure on the sides of the hull. The two main methods that are used for hull construction are: transverse framing and longitudinal framing. A system of ship construction in which the frames are closely spaced to furnish most of the strength to the ship's structure is called a transverse framing system. This type of framing is primarily used for ships of relatively short length (around 120 meters). In contrast, longitudinal framing is a very general term to identify any small longitudinal component that can be used for various purposes, and whose use is mandatory for very large ships (Okumoto et al., 2009). A schematic of hull structure is shown in Figure 1. It is obviously noticeable that the strength of the hull structure as a whole is maintained principally by the shear strength of its side shell plates, transverse bulkheads, and longitudinal bulkheads.

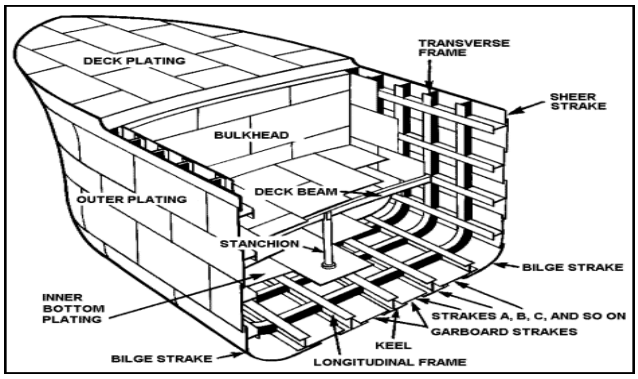

Figure 1: Main structural members of a ship hull

Source: (Military, 2013)

During its service life, a ship structure is subjected to numerous instances of severe loading. These loads can damage or weaken the structure as demonstrated in Figure 2. Hence, methods of repair or reinforcement to damaged or weakened parts of the structure for the purpose of restoring the structural integrity and thus assuring the ship's continued capability have become an important issue in recent years to military and civilian marine vessels alike (Sunyong Kim, 2010). The failure of a hull is induced by stress concentrations, which are caused by different types of loads acting on the hull. One category of hull failure is the development of large cracks that must be repaired for the ship to continue to be utilized. The principle of a bonded repair is shown in Figure 3. The commonly used composite patches and stiffeners have proved to be efficient and cost-effective repair methods that extend the durability and strength of damaged parts of marine structures and have several applications (Ting et al., 1999), (Hosseini-Toudeshky et al., 2012). There are many advantages to the use of composite patches as reinforcement to repair damaged hull structures, such as their light weight, resistance to

corrosion, and high strength and rigidity which conform to industry standards (Okafor et al., 2005).

The present study concerns the determination of the optimal orientation of the repair patch to reduce stress and strain concentrations in maritime vessel hull repair by implementing the Finite Element Method (FEM). Linear elastic stress analysis using ABAQUS/Standard V. 6.11 was conducted, and a finite element model was developed to study the effect of the composite patch orientations on an orthotropic stiffened hull. The goal is to reduce stress concentration by the use of orthotropic patches at specific orientations.

Figure 2: Damage to a ship hull

Source:(ASCHEMEIER, 2013)

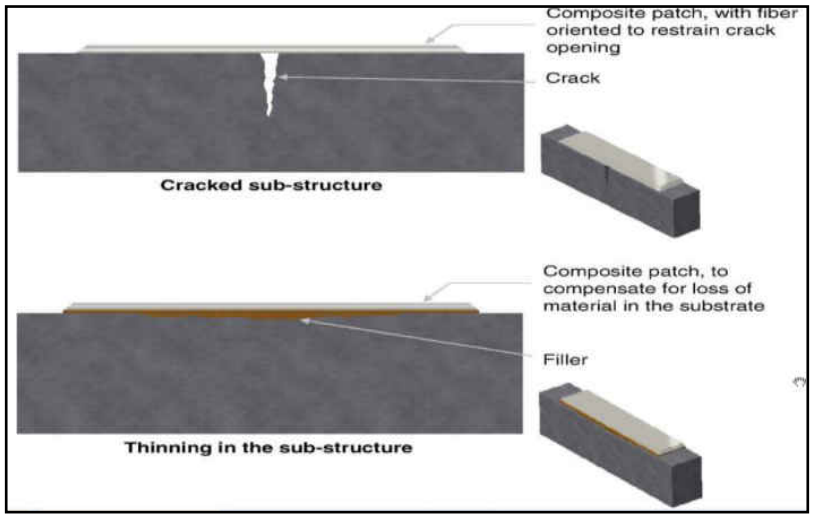

Figure 3: Concept of the composite repair for cracks

Source: (DNV-Standard, 2012)

CHAPTER 2: LITEARATURE REVIEW

The steel hull construction consists of stiffened panels, bottom construction, side shell construction, upper deck construction, bulkhead, as well as other parts. Stiffened panels consist of plates, beams and girders. The plates receive loads such as water pressure, while the beams support loads from the plates, and the girders support the loads from the beam (Okumoto et al., 2009). In most designs, the hull columns are cylindrical shells stiffened with both ring and longitudinal stiffeners; additionally, they are made rigid with web frames or transverse and longitudinal stiffeners (Demibilek, 1989). This structural complexity requires appropriate selection of design material, extensive welding, and maintenance procedures in case of hull failures.

The side shell of the hull structure provides defense against leakage of sea water when it is subjected to static sea pressure and dynamic effects of ship movement and wave actions in heavy weather. Figure 4 shows serious damage of a ship's sides as a result of these phenomena. In addition, aspects of the marine environment such as temperature and humidity may severely weaken the hull plating and stiffenersdue to different loading conditions acting on them. In general, hull repairs based on ABS standards are carried out by replacing the damaged areas with a patch of equal thickness,and stronger componets may support weakened stiffeners of the panel by applying connectingelements of the patch (ABS, 2007). In the past, traditional methods including gas heaters were used to control those conditions but were ineffective in changing the absolute humidity and simultaneously increasedenergy costs. Because of these conflicts, a new technology has been developed by Munter. With this technology, the absolute humidity can be decreased while heat increases. Some of the contributionsderived from the use of this technology

include uninterrupted work, reduced energy costs, and controlled resurfacing conditions (Munters).

The behavior of stiffened plates is affected by some important parameters, such as the length to width ratio of the panel, stiffener geometry and spacing, aspect ratio of plates between stiffeners, plate slenderness, vanishes stress, initial distortions, boundary conditions, and finally, types of loading (Amdahl, 2008).

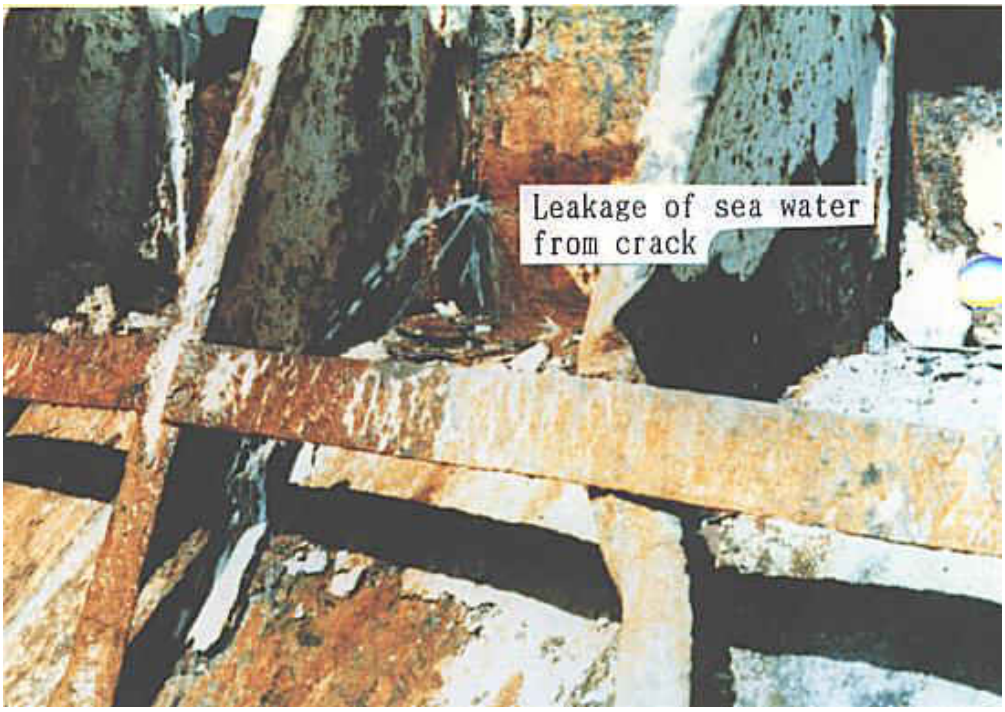

Figure 4: Leakage from side shell plating due to heavy corrosion

Source: (ABS, 2007)

Achieving ship durability and stability has been studied by many researchers, culminating in important contributions to improving ship-building industries. Steen (2013) assumed that there is another phenomenon that threatens the ship's overall integrity:fatigue failure. This failure is an integrated response effect over the lifetime of the ship which leads to cracks in the structure. Using Moore's law[1], computer hardware developments based on non-linear finite element analysis will lead to a doubling of the available calculation capacity every second year, so the time consumption in running analyses will be reduced. Another method for establishing the ultimate strength and reliability of a ship hull composed of orthotropic materials has been proposed by Chen et al. (2003). A composite column theory is used in this method. The method provides a quick and accurate solution to the collapse of composite stiffened panels, longitudinal ultimate strength, and reliability analysis of ship hulls. Also, Ziha et al. (2005) addressed the effects of hull deformations on ship displacement, which play an important role in the validation of a ship's operational efficiency. In addittion. They provided some assessment of the order of magnitude of the effect of bothlocal and global deformations based on the theory of isotropy and orthotropy.

As previously mentioned, the ship-building industry depends on the use of orthotropic panels because of their material properties. Many papers have been published which study the theories behind of the importance of these materials. Walsh et al. (2008) have studied the influence of slamming impact on orthotropic panels as compared to isotropic materials by using a linear-3D finite element analysis, which was performed for a spatially constant pulse model

[1]Moore's Law is a computing term which originated around 1970; the simplified version of this law states that processor speeds, or overall processing power for computers will double every two years.

and a traveling pulse mode. This study proved that composite panels behave differently from isotropic panels under slam loading. Thus, the dynamic analysis of a traveling pulse model is basically desirable for effective designs.

To evaluate the strength of stiffened panels, Assakkaf et al. (2008) have presented strength limit states for the different failure modes of ship panels. This study was important because of the influences of the three major types of loading that affect the strength of plate-stiffener panels. Load and resistance factor design (LRFD), which was derived from The First-Order Reliability Method (FORM) based on structural reliability theory, was the primary object of concern in this study. Soares et al. (1996) presented a formulation of the valuation of the fatigue reliability of ship hull girders. They studied the effects of a random number of cracks of different sizes in the longitudinal components of the midship to quantify the overall reliability of the hull. The formulation they studied was used for constant time intervals inspections; thus, the high reliability of repairs to be made on smaller cracks increases the reliability after repair.

The finite element method has been used for decades in solving many structural issues in different fields. In this study, a linear approach of a finite element analysis is used in the maritime vessel industry in order to determine the desired direction of the patch stiffeners such that stress resulting from the maintenance process will be less severe as well as less intense, and, as a consequence, the corrosion rate in the ship's hull structure will drop. If that is the case, the maintenance costs will decrease, and, moreover, the marine environment will be less vulnerable to risks arising from erosion of the ship’s hull.

Fundamentals of FEM are given by Okumoto et al. (2009) where the stiffness matrix and plane stress are considered. Since the ship contains thin plate structures, the examination is

applied to examples of plane deformation of plate elements in cases of linear stress analysis involving plane stress conditions in which the strains are constant in all directions. Modeling of a ship hull structure using FEA was employed by Zachariah et al. (1989). They completed a modeling of a hull with FEM in which the representation of the geometry, the accuracy of modeling of stiffness and strength of structural components of the hull depended on the analysis itself and the given conditions of the specific problems to be solved. For structural analysis of a composite hull structure, Ma et al. (2012) have developed a FE model, using sandwich construction in order to design a multi-hull ship structure. FE performs fluid structure interaction (FSI), which affects the structure response in cases of absence of coupling by FE.

Recently, the use of composite patches hasincreased in many industries for marine and aerodynamic applications among others. They showhigh sufficient strength to the structures to which they are applied. Repair of cracked parts of any structure by composite patches reduces the stress field near the crack by sealing the stresses between the cracked panel and the composite patch. Patch repair can be classified as temporary or permanent. In addition, patching methods are used to improve the strength of an existing undamaged structure to enable it to support more substantial loadings and overcome any design weaknesses (Halliwell, 2007). Another contribution to ship hull repair was made by Grabovac et al. (2009), who studied the technology of carbon reiforcement to repair cracked ship panels. Their study proved the suitability of using composite patches for marine structure repair because no cracking has occurred in the repaired regions over 7 years later. The use of adhesively bonded steel and carbon reinforcements have been found to be superior both for static strength and behavior under fatigue.

In order to minimize the severe conditionscaused by the mismatch that occurs if the material properties of the patch as well as the panel are the same duringpatching process, it is necessary that the patch be morerigid than the stiffened panel. Also, it is suggested to add an isotropic layer to the interaction to decrease the severeity of these stresses. This can be achieved by determining the equivalent orthotropic properties from the isotropic properties of each. This study will consider such an example of structurally orthotropic plates.

Forming or shaping a normally isotropic material to produce the required orthotropic properties has been widely studied by many researchers, especially in infrastructure fields. One example of such usage involves steel corrugarted sheets. Analytical development in the determination of orthotropic properties of steel plates derived from the isotropic properties of steel was presented by Ahmed et al. (2003). In addition, they contributedan evaluation of the ability to predict the behavior of any structure that contains such anisotropic properties. Theyapplied the method of elastic equivalence to the analysis of the corrugated steel sheets in a2-D orthotropic plate as shown in Figure 5. They assumed that the equivalent 2-D orthotropic plate has a constant thickness and the same length as well as width of the profiled sheeting, and each element of the plate behaves as a shell element having different moduli both in-plane and out-of plane in the two principal directions. Their study showed that idolization of deriving the orthotropic properties of the corrugated sheets is capable to predict its structural behavior and response.

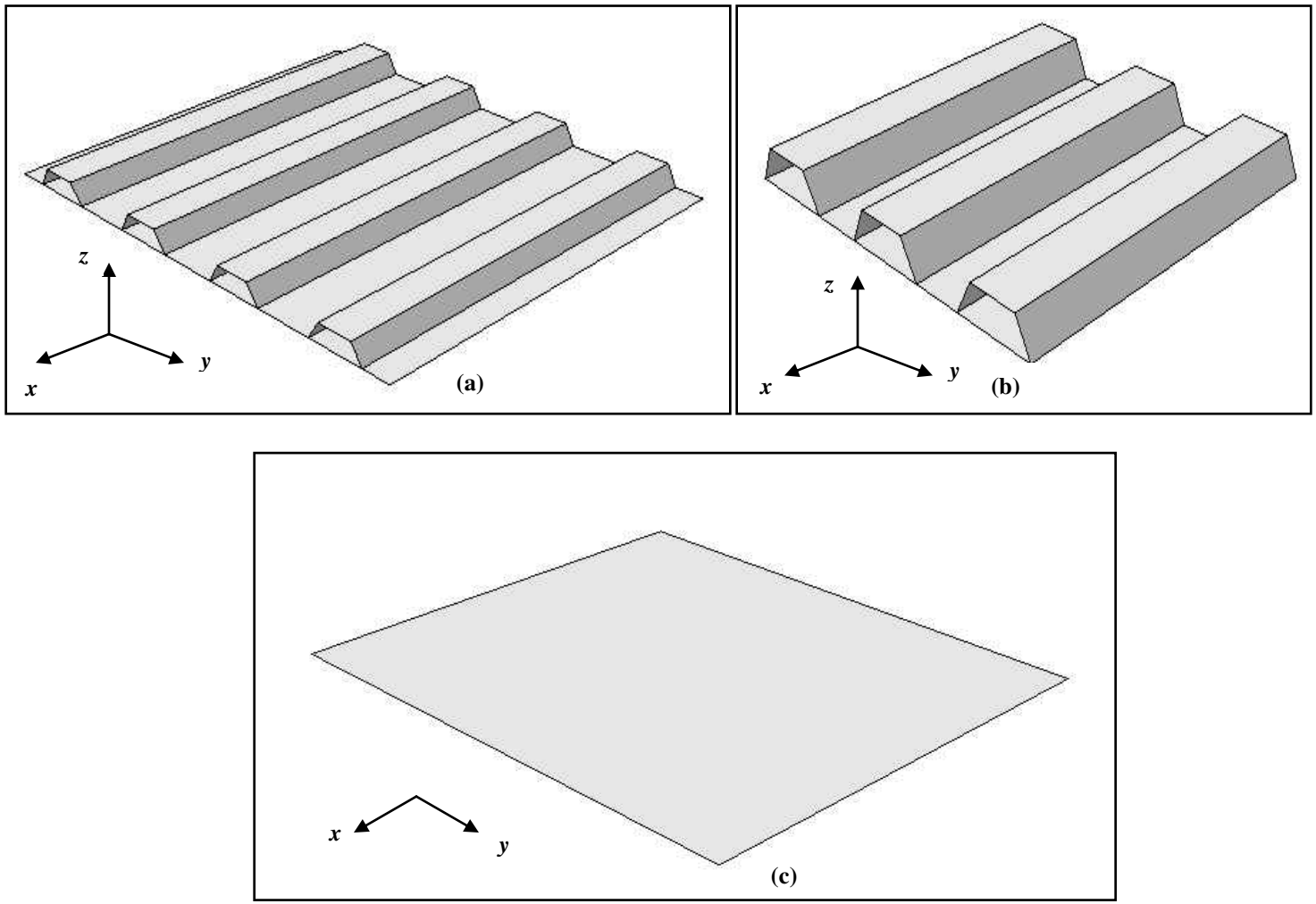

Figure 5: Method of Elastic Equivalence. (a) Original Stiffened Panel, (b) Original Stiffened Patch

(c) Equivalent Orthotropic Plate

Another study was presented by Wennberg et al. (2011) in order to reduce the required number of elements in FE by replacing the corrugated sheet with a 2-D orthotropic model. They studied the corrugated steel sheet in three modes, vibration, extension, and buckling, using FE software with three different methods of calculation that were computed by three reserchers. In addition tothe model produced by Wennberg et al. (2011), another finite element model of bridge corrugated sheets with equivalent orthotropic material has been presented by Zhang et al. (2013). They presented a multiple scale modeling and simulation scheme basedon an equivalent orthotropic material modeling (EOMM) method capable of including refinedstructural details. Bridge details with complicated multiple stiffeners weremodeled as equivalent shell elementsusing equivalent orthotropic materials, resulting in the same longitudinal and lateral stiffness inunit width and shear stiffness in the shell plane as the original configuration. Based on the multi-scale modeling method, it is possible to predict a reasonable static and dynamic response of the bridge details since the (EOMM) model is able to include the global vibration modes and local vibration modes of the original model with refined structural details. Moreover, it is possible to calculate the dynamic effects in multiple scales, namely from the wind loads in a low frequency region if enough global vibration modes are included, and from the vehicle loads in a meter scale in a high frequency region if enough local modes are included in the analysis.

CHAPTER 3: FINITE ELEMENT ANALYSIS

Introduction

Due to different orientations in anisotropic metal plates, there can be additional stress and strain concentrations that occurr at the interaction layer between the ship hull and the patch. Therefore, the patch can be set at different degrees of inclination to the original orientation of the hull, and evaluated via finite-element simulation. An optimization procedure will aim to reduce the stress around the patched area of the hull panel. The simultaneous effect of both the shape and the orientation of the patch can coexist. Here, the repair of ship structures with patches having orthotropic properties is carried out using ABAQUS. The following section describes the use of this method to repair a damaged hat-stiffened hull panel.

As hull strength assessment is based on the strength of stiffened panels, the modeling of the ship's cross section consists of discretizing the hull into stiffened plate elements which are representative of panel behavior. The design philosophy of the ship-building industry is oriented mainly to longitudinal stiffened hulls. In these hulls, it is currently common practice to have panels with similar and repetitive properties such as space between stiffeners, thicknesses, and stiffener geometry. As the behavior of these panels may be represented by the behavior of unequally stiffened plate elements, the hull section will be divided into small elements representing a plate between stiffeners and the corresponding stiffener (PG, 2008).

This chapter presents a description of the developed finite element model to determine the effect of different patch orientations on the hull frame.

The Finite Element Model

Modeling the hat-stiffenedplate using shell elements is complex, especiallyregarding how to connect the stiffenerswith the plate. Clearly, the middle surface of theplate does not correspond with that of the stiffenerflanges, as can be seen from Figure 6b. In view of the fact that only thenodal points within the central surfaces are defined,the stiffener flanges cannot be linked to the plateexactly by using common nodal points at theboundary. Theapproach in modeling the hat-stiffened plate is to simplify the geometry of the corrugated steel sheeting plates, the panel, and patch,as shown in Figure 5, to 2-D shell element. Where the panel has 4 stiffeners with 350 mm spacing, the patch has 3 stiffeners that are 150 mm apart.The analysis was done by applying the equivalent orthotropic theory of corrugated plates.

As is known, shell elements are used to model structural elements in which two dimensions are much greater than the third, and the change of the analyzed feature across the third can be neglected. The advantages of the use of shell elements result mainly in saving time due to the reduced number of finite elements.

A numerical model has been created and analyzed using the commercial finite element code ABAQUS/Standard Version 6.11. In this study, a 2-D conventional planar shell element was used to model the hull of the ship, the panel, patch, and isotropic contact layer. As a result of severe conditions of high stress and strain levels that occur at the interface between the panel and patch, it is significant to add an interface layer with isotropic properties in order to reduce the stress and strain concentrations.

The length and width of the stiffened panel are denoted by L and W, respectively. The thickness of the plate is t. The model was made of Mild Steel (ASTM A131AH36) having a

thickness of 6 mm. The geometrical dimensions are: a panel of 2800×2400 mm, a patch of 1050×1050 mm, and an interface layer of 1080×1080 mm with a thickness of 6 mm, as shown in Figures 7, 8, and 9.Hat-stiffeners were made of mild steel as well. The cross-sectional geometry of hat-stiffened panelsfeaturing four stiffeners and its dimensions are given in Figure 6 .

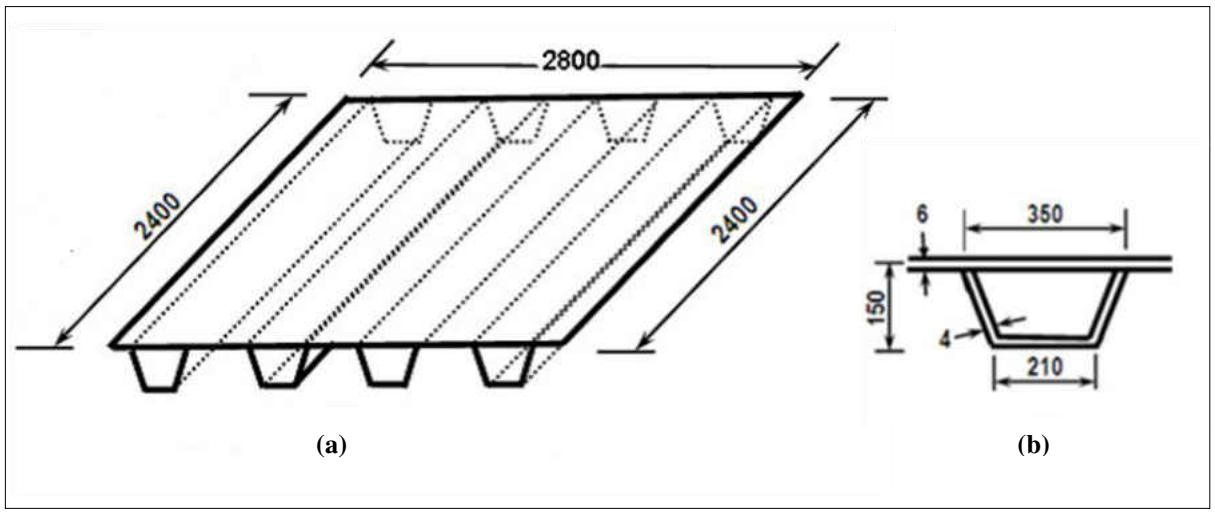

Figure 6: (a) Illustration of geometry and dimensions of hat stiffened plate having four stiffeners, (b) The principle dimensions of the hat stiffener

Source: (Tharian et al., 2013)

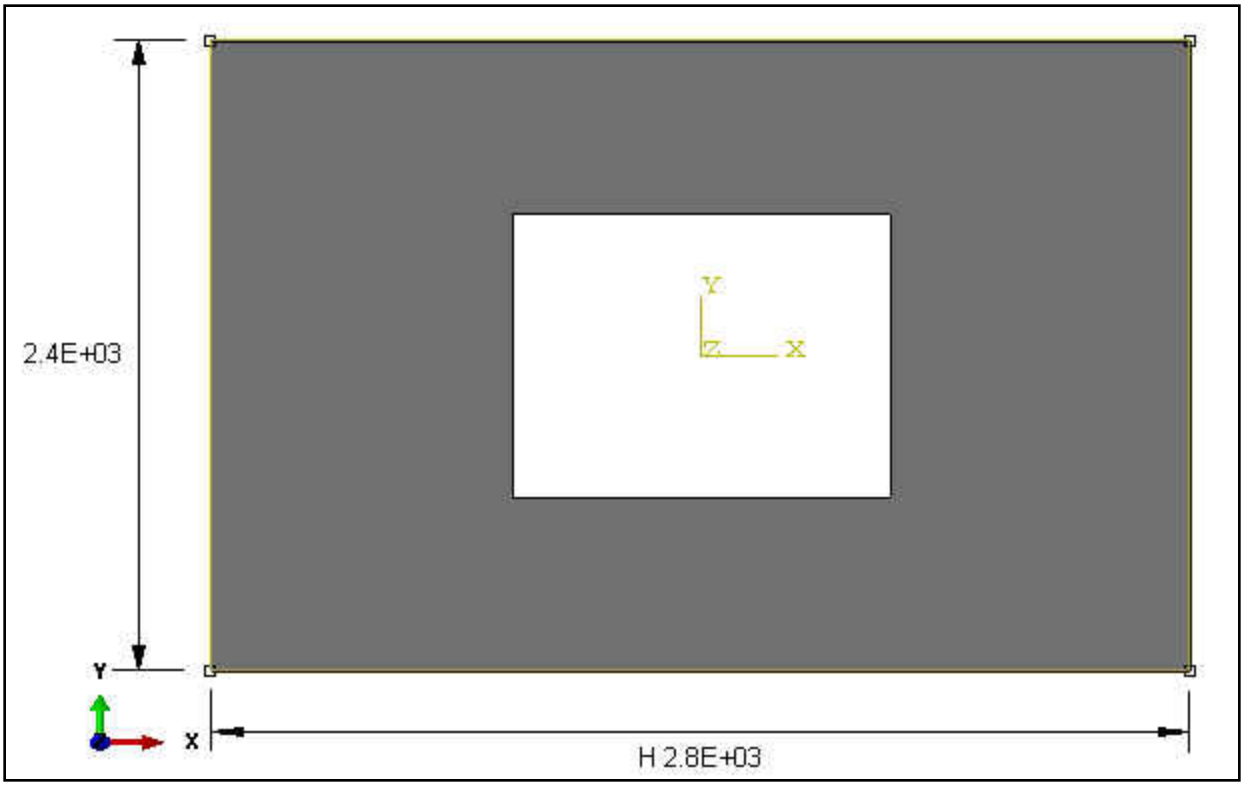

Figure 7: Panel geometry with damaged section removed

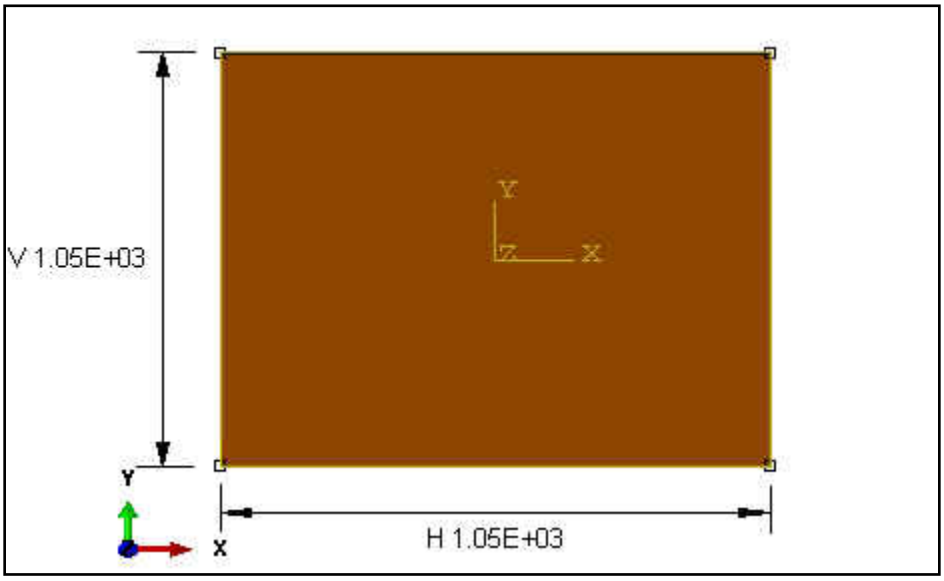

Figure 8: Anisotropic patch geometry

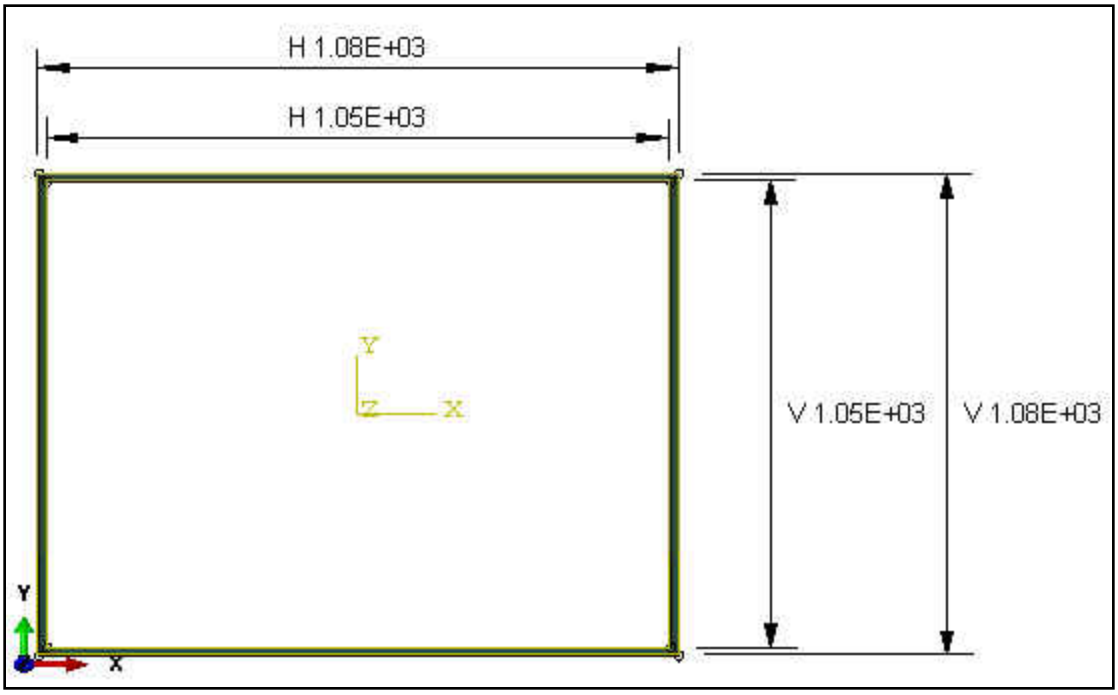

Figure 9: Isotropic layer geometry

Material Properties

An elastic material model with a vonMises yield criterion was used to model the material's constitutive behavior. The chemical components and the mechanical properties of the mild steel or ship-building steel plates (ASTM A131 AH36) are given in Tables 1 and 2 respectively.

Table 1: AH36 Steel Plate Chemical Composition %

Grade	C max	Si max	Mn	P max	S max	Al min	Ti max	Cu max	Cr max	Ni max	Mo max	Nb	V
AH36	0.18	0.5	0.90-1.60	0.035	0.035	0.015	0.02	0.35	0.2	0.4	0.08	0.02-0.05	0.05-0.10

Source: (BEBON, 2011).

Table 2: Mechanical Properties of AH36 steel plate

Grade	Tensile strength (σ_T, MPa)	Yield stress (σ_y, Mpa)	Young's modulus (E, GPa)	Poisson's ratio (ν)	Density (ρ, g/cm^3)
AH36	490-630	355	210	0.3	7.85

Source: (BEBON, 2011).

Mesh, Geometry and Boundary Conditions

The model of the whole structure is established using finite element analysis S4R from ABAQUS software. S4R element is a 4-node, quadrilateral, stress/displacement shell element with reduced integration and a large strain formulation. The element has six degrees of freedom at each node and the corresponding nodal displacements are (Abaqus, 2011),

$$\{U\} = \{u_1\ u_2\ u_3\ UR_1\ UR_2 UR_3\}$$

S4R elements offer many advantages, such as the reduced integration of isoparametric elements which compute strains and stresses at locations known to provide optimal accuracy. Thus, reduced integration softens the response of the elements, which leads to increased accuracy by resisting the overly stiff response generally encountered in FEA. In addition, the use of fewer elements benefits the user with reduced computing time and storage requirements (Cullen, 2007).

The FE model is shown in Figure 10. This model consists of 622S4R element shell elements in the panel, 121 elements in patch, and 928 nodes. An isotropic four-node shell element was used in the analysis to model the steel layer with 44 elements and 88 nodes.

Bysetting the boundary conditions and contact forces, the different components are meshed using corresponding element types. The detail is given in Table3.

Table 3: Mesh Element Description

NO.	Element type	Element description	Material	Number
1	Shell S4R	Panel	Equivalent orthotropic properties of AH36 steel	622
2	Shell S4R	Patch	Equivalent orthotropic properties of AH36 steel	121
3	Shell S4R	Interface Layer	Isotropic properties of AH36 steel	44

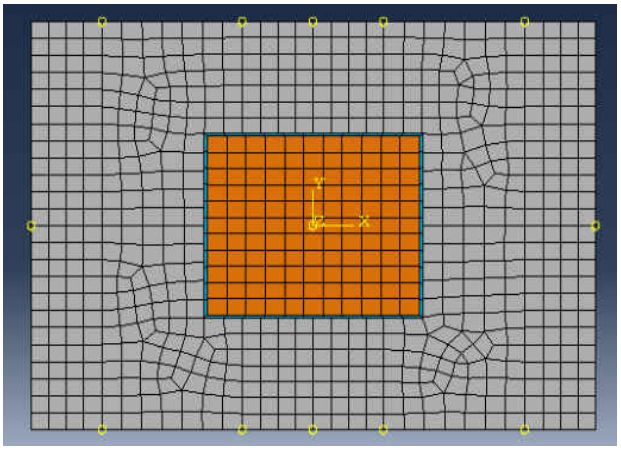

Figure 10: FEM mesh of the ship hull model

Three sets of boundary conditions were defined. One is simply a supported boundary condition on all four edges, a uniformly distributed lateral pressure of 0.2 MPa, corresponding to a 20 m water column (Byklum et al., 2004) which has been applied to the hull, and a value of 2.029 mm displacement load in y-direction (U_2) was applied on the direction of the stiffeners of the panel (corresponding to axial force of 15 kN in the direction of stiffeners). The spatial and rotational displacements (U_3 and UR_3) around the z-axis are fixed along all edges, and the displacements U_1 and UR_1(spatial and rotational displacements around the x- axis) are also constrained for left and right edges, while $UR_2$is left unconstrained to allow rotation around the y-axis. For the top and bottom edges, U_2 is left unconstrained as well. This is because the load is applied in this direction and from those edges as previously mentioned.

Furthermore, displacement control has been considered as an equivalent force. Displacement control, however, is known as displacement loading in which the loads are applied to a specific part of the model. In a displacement controlled analysis, the displacement changes

incrementally. A reaction force is best thought of as the force required to apply a particular displacement (Milligan, 2012). Figure 11 shows the boundary conditions for the ship hull model.

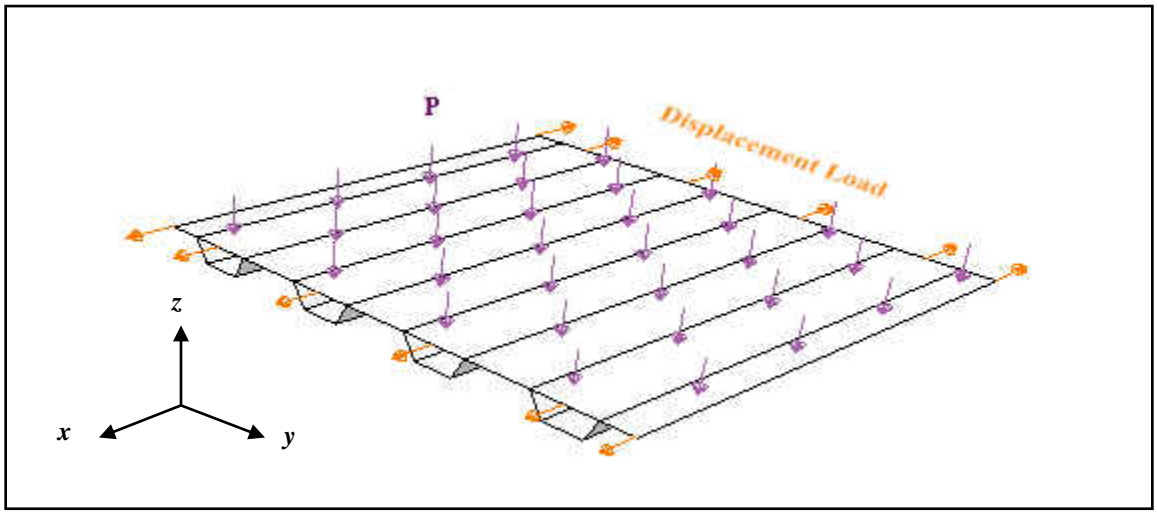

Figure 11: The hull model under uniform pressure (P) and uniaxial tension of a displacement control.

The value of the displacement load (U_2) is taken to be a reasonable proportion of the yield strain, for example 50%. So, there is no possibility of yielding to occur.

From Hooke's law as given in Equation 1,

$$\Delta U = \frac{\sigma}{E} L \qquad (1)$$

Where σ is the tensile stress, E is the Young's modulus of the mild steel, and L is the total length.

Taking ΔU to be U_2, and σ to be σ_y, hence;

$$U_2 = \frac{355 \times 50\%}{210 \times 10^3} \times 2400 = 2.029\ mm$$

This displacement loading is equivalent to a control force loading of 15 kN that is applied along the stiffeners of the panel.

The model was assembled and a general static (STEP) option was used for the analysis in ABAQUS code. Only linear effect was included in this analysis. Automatic increment of the static step was used with a maximum number of 10^7. Minimum increment size was 10^{-30}. The maximum increment size was used with a value of 1. Also, direct equation solver method was used.

A surface to surface tie constraint was created to tie the model. This type of constraint allows fusing together two regions even though the meshes created on the surfaces of the regions may be dissimilar (Abaqus, 2011). Figure 12 demonstrates the tie constraints that were created to tie the hull model. As shown, the green boundaries represent the tie constraint for bonding the panel boundaries with the outer surfaces of the interface layer, whereas the red boundaries show the tie that was created to fuse together the patch boarders with the inner surfaces of the interface layer.

In order to study the effect of patch orientation on reducing the stress and strain levels on the hull model, 3 different orientation angles for the patch were considered. Figure 13 shows the corresponding axes for the material orientation of the patch.

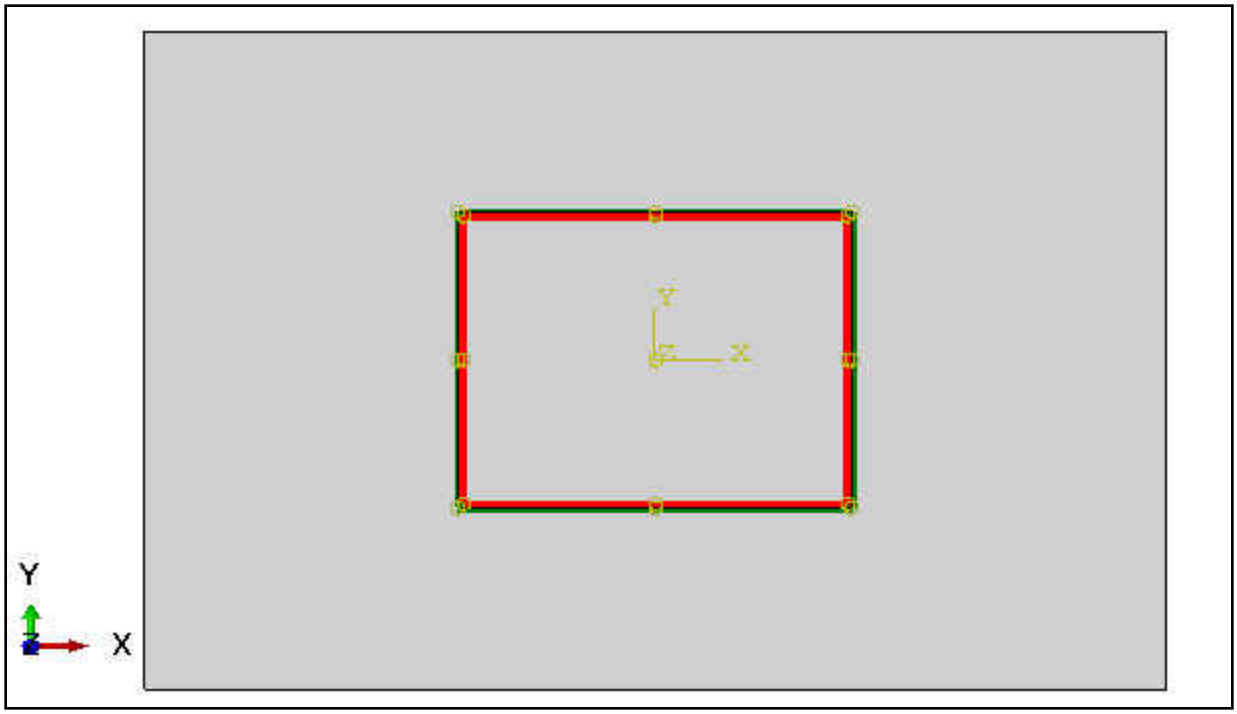

Figure 12: Tie constraint for the FE model

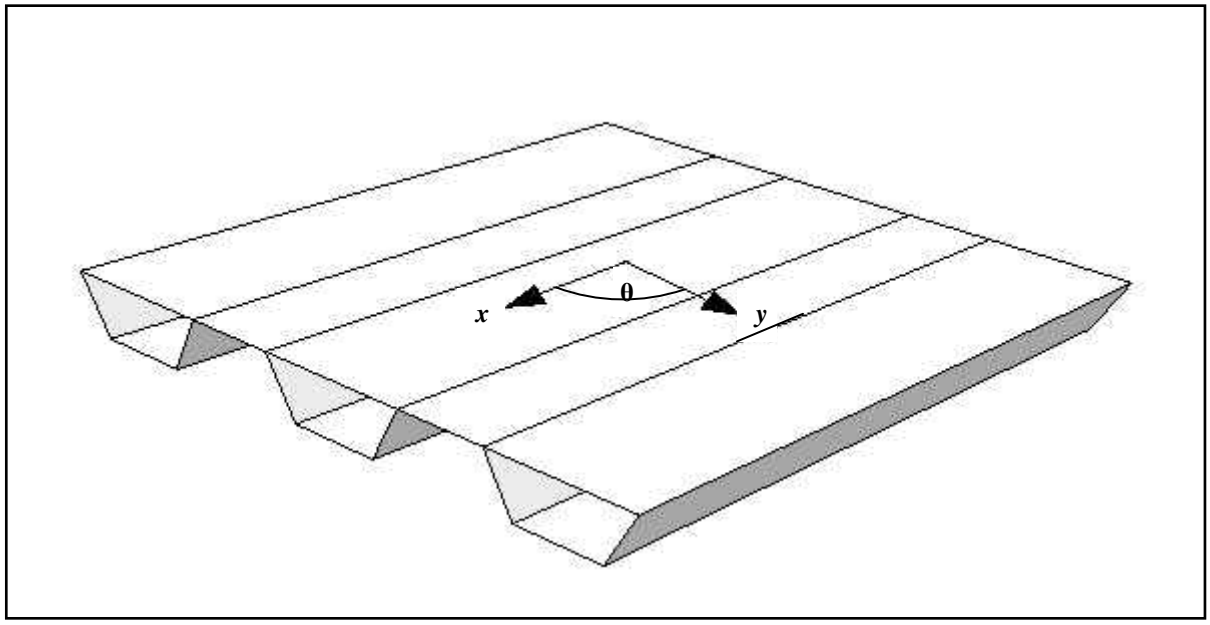

Figure 13: Patch material orientation at the corresponding axes

Solution Strategy

ABAQUS uses elasto-static stress procedure in which inertia effects are neglected for predicting the material and geometric linearity. Linear static analysis involves the specification of load cases and appropriate boundary conditions. If all or part of a problem has linear response, substructuring is a powerful capability for reducing the computational cost of large analyses (Abaqus, 2011).

For most of the repaired panels with properly prepared patches before repair, there was a small discontinuity area in a small area around the damaged area. It is worth mentioning that, in the FEM modeling of this study, a small discontinuity area between the patch and panel interaction has been considered. A comperhensive finite element analysis of the ship hull has been performed using the elastic solution of ABAQUS finite element code.

Two cases are studied and analyzed. In the first case, all elastic and shear constants for the panel and patch are different although both are made of the same material. In this case (Case 1), the patch requires to be stiffened more than the panel to strengthen the repaired region. Conversely, in the second case, the values of Young's and Shear Moduli are equal. The material of the interface layer is isotropic mild steel. The purpose of this analysis is to study the effect of patch orientations in reducing the stress and strain concentrations at the area of interaction in both cases. By way of explanation, the analysis will examine whether the model requires stiffer properties of patch than are in the panel to obtain one of this study's goals.

The panel edges are considered to be simply supported. A combination of uniaxial tension loads and lateral pressure have been applied on the hull model. An equivalent displacement loading of 2.029 mm (equivalent to axial force of 15 kN) was applied along stiffener directions on the equivalent panel, and the model was subjected to a hydrostatic pressure of 0.2 MPa.

CHAPTER 4: RESULTS AND DISCUSSIONS

Calculations

Applying the equivalent orthotropic theory of corrugated plates which was presented by Ahmed et al. (2003), the resulting expressions of Young's modulus in the x and y axes are given in Equations 2 and 3 respectively. Also, the calculation of the effective shear modulus of the equivalent plate for the corrugated steel sheeting is given in Equation 6. The procedure that was followed to establish the equivalent orthotropic properties was done by applying an axial load to the sheet ends and taking the x-axis to be oriented parallel to the sheet corrugation for calculating E_x. And for calculating E_y, the load should be parallel to the y-axis (Ahmed et al., 2003).

$$E_x = E_0 \frac{s}{d} \tag{2}$$

$$E_y = E_0 \frac{I_0}{I_x} d, \; I_0 = \frac{t^3}{12} \tag{3}$$

And Poisson's ratio in-plane x and y directions consequently are given in Equations 4 and 5 as;

$$\nu_x = \nu_o \tag{4}$$

$$\nu_y = \nu_o \frac{E_y}{E_x} \tag{5}$$

Where, E_0 and ν_0 are Young's modulus and Poisson's ratio of the Mild-Steel (ASTM A131 AH36); *d* is the wave length (pitch) of the corrugation (see Figure 33 in Appendix A), *s* is the original width of the corrugation before deformation occurs, *t* is the thickness of the profiled

sheeting, and I_x is the second moment of inertia of one repeating section of corrugation about the normal axis.

$$G_{xy} = \frac{G_0 t}{\frac{s}{d} + \frac{d^{2.5}\overline{K}}{2(1+\nu_0) l_a t^{1.5}}} \quad (6)$$

Where,

$$G_o = \frac{E_o}{2(1+\nu_o)} \quad (7)$$

Where, G_0 is the shear modulus, l_a is the the length along the corrugation, and $\overline{K}$ is a dimensionless constant for sheet distortion. This constant depends on the following factors: the ratio between the profile dimensions and the pitch of corrugations ($\frac{2b_T}{d}$), the angle Theta (θ), and the ratio between the height of sheeting profile and the pitch of corrugations (h/d). as shown in Figure 37 in Appendix B (Davies et al., 1978).

Calculations of the Equivalent Orthotropic Properties of the Panel

The first part of the calculations is to determine the moment of inertia of one repeating section of corrugation about the neutral axis (I_x) of the profiled steel plate as shown in Figure 34 in Appendix A. Using Equations 8 and 9 below; I_x is found to be 19.212×10^6 mm^4. All the calculations for finding I_x have been performed as in Greene (1999). Table 4 shows the procedure of I_x through its calculations.

Table 4: Calculations of the second moment of inertia at the neutral axis for the panel

Item	b (mm)	h (mm)	A=b×h (mm^2)	d (mm)	d^2 (mm^2)	Ad (mm^3)	Ad^2 (mm^4)	$I_\circ=\frac{bh^3}{12}$ (mm^4)
A	210	4	840	146	21316	122640	17905440	1120
B1	4	156.53	626.12	75	5625	46959	3521925	1278413.95
B2	4	156.53	626.12	75	5625	46959	3521925	1278413.95
C	700	6	4200	3	9	12600	37800	12600
Total			6292.24			229158	24987090	2570547.9

$$\bar{Y} = \frac{\sum Ad}{\sum A} \quad (8)$$

$$\bar{Y} = \frac{229158}{6292.24} = 36.42\ mm.$$

$$I_x = \sum I_o + \sum Ad^2 - [\sum A \times \bar{Y}^2] \quad (9)$$

$I_x = 2570547.9 + 24987090 - [6292.24 \times 36.42^2]$. Hence; $I_x = 19.212 \times 10^6\ mm^4$

All modulus; E_x, E_y, and G_{xy} will be calculated for one repeating section of the plate. The profiled plate will be assumed to be fastened in every corrugation. From Figure 35 in Appendix A, *d* is calculated to be 700 mm, *s* = 891.06 mm, *t* = 6 mm.

Now, from Equation 2,

$$E_x = E_0 \frac{s}{d} = 210 \times 10^3 \times \frac{891.06}{700} = 267.318\ GPa$$

And, from Equation 3,

$$E_y = E_0 \frac{I_0}{I_x} d = 210 \times 10^3 \times \frac{6^3}{12} \times \frac{700}{19.212 \times 10^6} = 137.73 \times 10^{-3}\ GPa$$

From the calculations of E_x and E_y, it is obvious that E_x is nearly 2×10^3 orders of magnitude greater than E_y. This would be significant to the application of the equivalent orthotropic properties of the corrugated plates.

The values of the in-plane Poissons ratio are found from Equations 4 and 5 respectively as follows:

$$\nu_x = \nu_o = 0.3$$

$$\nu_y = \nu_o \frac{E_y}{E_x} = 0.3 \frac{137.73}{267318} = 0.00015$$

As mentioned earlier, the value of $\overline{K}$ can be found in Figure 38 in Appendix B. Consequently, $\overline{K}$ = 0.127 which will be used for calculation. From Equation 7, the value of G_o is determined to be,

$$G_o = \frac{E_o}{2(1+\nu_o)} = \frac{210 \times 10^3}{2(1+0.3)} = 80.76923\ GPa$$

Therefore, for a 2800 mm span (l_a) and from Equation 6,

$$G_{xy} = \frac{G_0 t}{\frac{s}{d} + \frac{d^{2.5}\overline{K}}{2(1+\nu_0) l_a t^{1.5}}} = \frac{80769.23 \times 6}{\frac{891.6}{700} + \frac{700^{2.5}(0.127)}{2(1+0.3)2800 \times 6^{1.5}}} = 24.74\ GPa$$

Calculations of the Equivalent Orthotropic Properties of the Patch

The same equations and procedure have been followed for finding the equivalent orthotropic properties of the patch. Table 5 demonstrates the calculation of the second moment of inertia about its neutral axis.

Table 5: Calculations of the second moment of inertia at the neutral axis for the patch

Item	b (mm)	h (mm)	A=b×h (mm^2)	d (mm)	d^2 (mm^2)	Ad (mm^3)	Ad^2 (mm^4)	$I_\circ = \frac{bh^3}{12}$ (mm^4)
A	100	4	400	110.184	12140.51386	44073.6	4856205.542	533.33
B1	4	121.8	487.2	65	4225	31668	2058420	602310.744
B2	4	121.8	487.2	65	4225	31668	2058420	602310.744
C	400	6	2400	3	9	7200	21600	7200
Total			3774.4			114609.6	8994645.54	1212354.82

From Equation 8,

$$\bar{Y} = \frac{\sum Ad}{\sum A} = \frac{114609.6}{3774.4} = 30.365\ mm$$

And then, from Equation 9,

$$I_x = \sum i_0 + \sum Ad^2 - \left[\sum A \times \bar{Y}^2\right] = 1212354.821 + 8994645.542 - [3774.4 \times 30.635^2]$$

$$= 6.729 \times 10^6\ mm^4$$

From Figure 36 in Appendix A, *d* is calculated to be 400 mm, *s* = 510 mm, *t* = 6 mm.

Now, from Equation 2,

$$E_x = E_0 \frac{s}{d} = 210 \times 10^3 \times \frac{510}{400} = 267.75\ GPa$$

And, from Equation 3,

$$E_y = E_0 \frac{I_0}{I_x} d = 210 \times 10^3 \times \frac{6^3}{12} \times \frac{400}{6.729 \times 10^6} = 224.77 \times 10^{-3}\ GPa$$

As seen from the calculations of Young's moduli, E_x is approximately 10^3 greater than E_y. As stated previously, this significant magnitude is important for the plate to follow the equivalent orthotropic approach.

Now, from Equations 4 and 5,

$$\nu_x = \nu_o = 0.3$$

$$\nu_y = \nu_o \frac{E_y}{E_x} = 0.3 \frac{224.77}{267750} = 0.00025$$

From Figure 39 in Appendix B, the value of $\overline{K}$ is interpolated to be 0.168. Hence; for a 2400 mm span (l_a) and from Equation 6,

$$G_{xy} = \frac{G_0 t}{\frac{s}{d} + \frac{d^{2.5}\overline{K}}{2(1+\nu_0) l_a t^{1.5}}} = \frac{80769.23 \times 6}{\frac{510}{400} + \frac{400^{2.5}(0.168)}{2(1+0.3)2400 \times 6^{1.5}}} = 28.37GPa$$

The following table tabulates the equivalent material properties of the panel and patch that were established previously:

Table 6: In-plane properties of equivalent orthotropic plate

Material Property	E_x (MPa)	E_y (MPa)	G_{xy} (MPa)	ν_x	ν_y
Panel	267318	137.73	24739.89	0.3	0.00015
Patch	267750	224.77	28367.25	0.3	0.00025

From the calculation results, it is observed that for a plate (either panel or patch) having shorter l/d ratio (i.e. span less than 2800 mm), the 2-D equivalent orthotropic approach was applicable and gave satisfactory results. This can be seen from the calculations for the equivalent Young's moduli for the patch.

Results

This section summarizes the results of the FEA for the ship hull. For validation of the developed computational model, analyses were performed using the linear finite element code ABAQUS/Standard V. 6.11.

The stress and strain distribution of various patch orientations at the panel-interface layer-patch assembly computed using finite element analysis. These stresses and strains can be significantly decreased by the effect of an equivalent orthotropic patch. These stress and strain values will be checked against the values obtained from Case 2 for the non-repair panel in order to validate the hypothesis of different patch orientations. The von Mises stresses and strains at the connection area are then studied individually at each orientation angel to ascertain the strength, durability and effectiveness of the patch repair.

The main objective is to obtain the optimum orientation of the patch repair that allows for reduction of the stress and strain concentrations after repair, for both the cases prescribed earlier in Chapter 3.

Effect of Patch Orientations

In this section, effects of equivalent orthotropic patch orientations on reducing the stress and strain levels, and hence stress and strain concentrations, around the interaction area between the panel and patch of both aforementioned cases are analyzed. For this purpose, repaired panels with 350 mm stiffeners spacing and three different patch orientation angles of 0°, 45° and 90° are considered. Determining the optimum patch orientation was done by selecting the maximum value of von Mises stress and strain concentrations on each region of the model at different orientation angels, and then those results were graphically represented.

Stress and Strain Analysis at the Boundaries

The von Mises stress and maximum principal strain are computed on the boundary for different patch orientations, and are shown in Figures 14 and 15. Their minimum values occur when the orientation angle is 0°. The difference between the obtained stresses and strains at the interface layer under both cases is demonstrated in Table 7. The von Mises stress of the interface layer is 123 MPa, for the case in which the patch is stiffer than the panel, refers to solution strategy in Chapter 3. It is the same for the second case when the material constants for the panel and patch are equal. These values are less than the yield stress of the used material, which led to elastic deformation at the bonded line. It is evident that there is no significant impact of the patch on the stress and strain distributions on the bonded area by changing the material properties of the patch at a rotation angle of 0° in both cases of study.

In addition, for 45° and 90° orientations, the stress and strain are critical and intensively increasing, especially at a patch orientation of 45°.

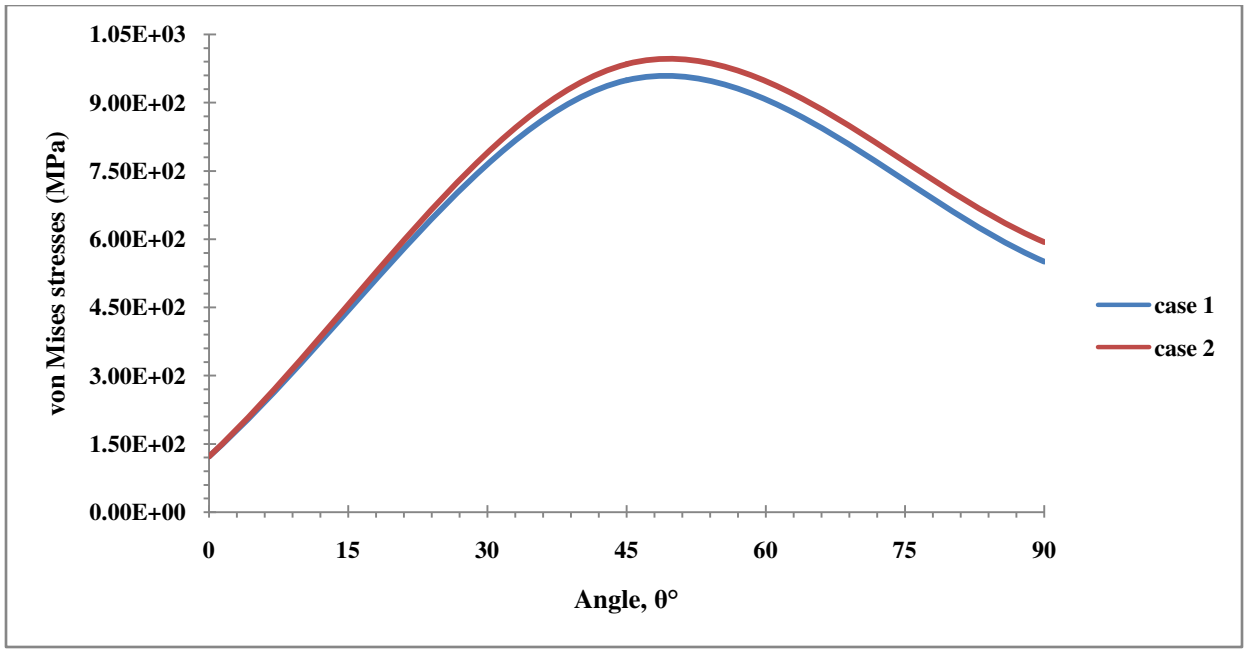

Figure 14: Stress concentrations at the boundary

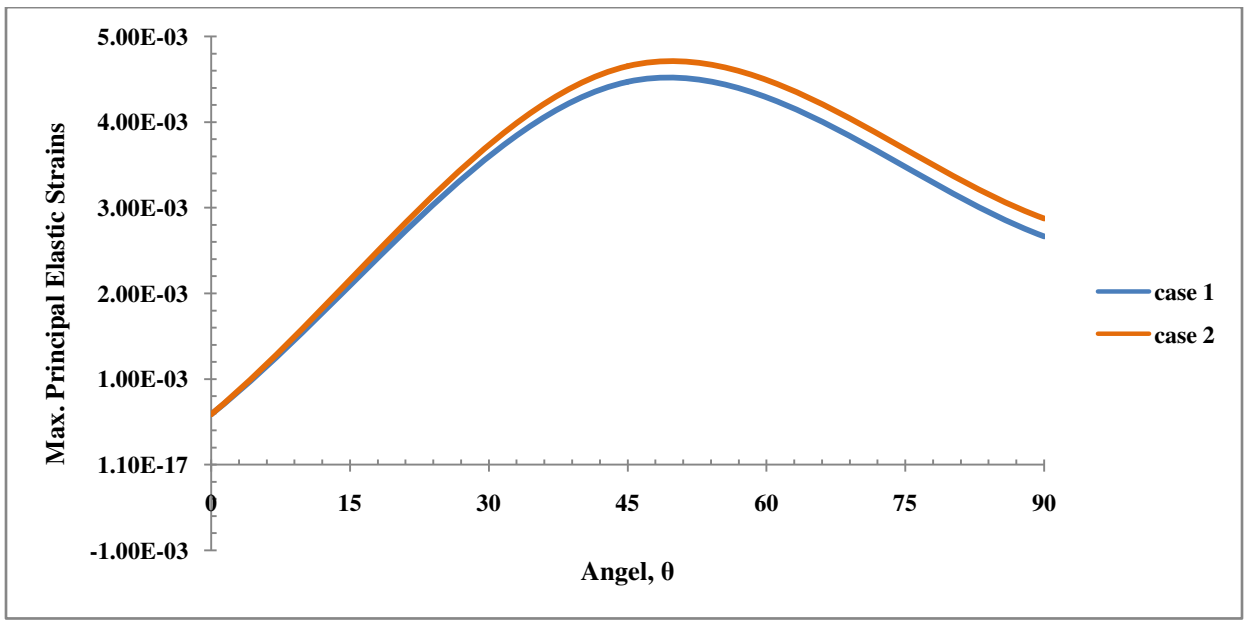

Figure 15: Elastic strain concentrations at the boundary

Table 7: Results and comparisons of stress and strain distributions at the boundaries

Angel, θ°	Case 1	Case 2
	Equivalent Stresses (von Mises, MPa)	
0	1.23E+02	1.23E+02
45	9.49E+02	9.85E+02
90	5.50E+02	5.94E+02
Angel, θ°	Maximum Principal Elastic Strains	
0	5.87E-04	5.88E-04
45	4.47E-03	4.65E-03
90	2.67E-03	2.87E-03

Comparing Stress and Strain Distributions on the Hull Regions

As expected, the patch orientation affects the stress and strain distribution and concentration at the boundary. The results presented in Figures 16 and 17 show that stress and strain distributions are critical to occur at the boundaries for all orientation angles: 0°, 45° and 90°, in each case. Moreover, it would be significant to use the obtained results to determine which are needed to reduce the required level of stress in a desired part of the structure. However, it is worthwhile noting that the 0° angle reduces the stress on the boundaries just below 123 MPa and with a minimal increase of stress on the repaired panel.

Studying and comparing the effect of the patch orientations on the two regions of the ship hull, the panel, and the interface layer, as illustrated in Tables 8 and 9, it is evident that the area

at the interaction considerably reduced the severity conditions of stress and strain concentrations that would occur.

Table 8: Results and comparisons of stress and strain distributions of the hull model under case 1

Angel, θ°	Equivalent Stresses (von Mises, MPa)	
	Interface Layer	Panel
0	1.23E+02	1.24E+02
45	9.49E+02	3.64E+02
90	5.50E+02	3.62E+02
Angel, θ°	Maximum Principal Elastic Strains	
	Interface Layer	Panel
0	5.87E-04	1.38E-02
45	4.47E-03	4.13E-02
90	2.67E-03	3.15E-02

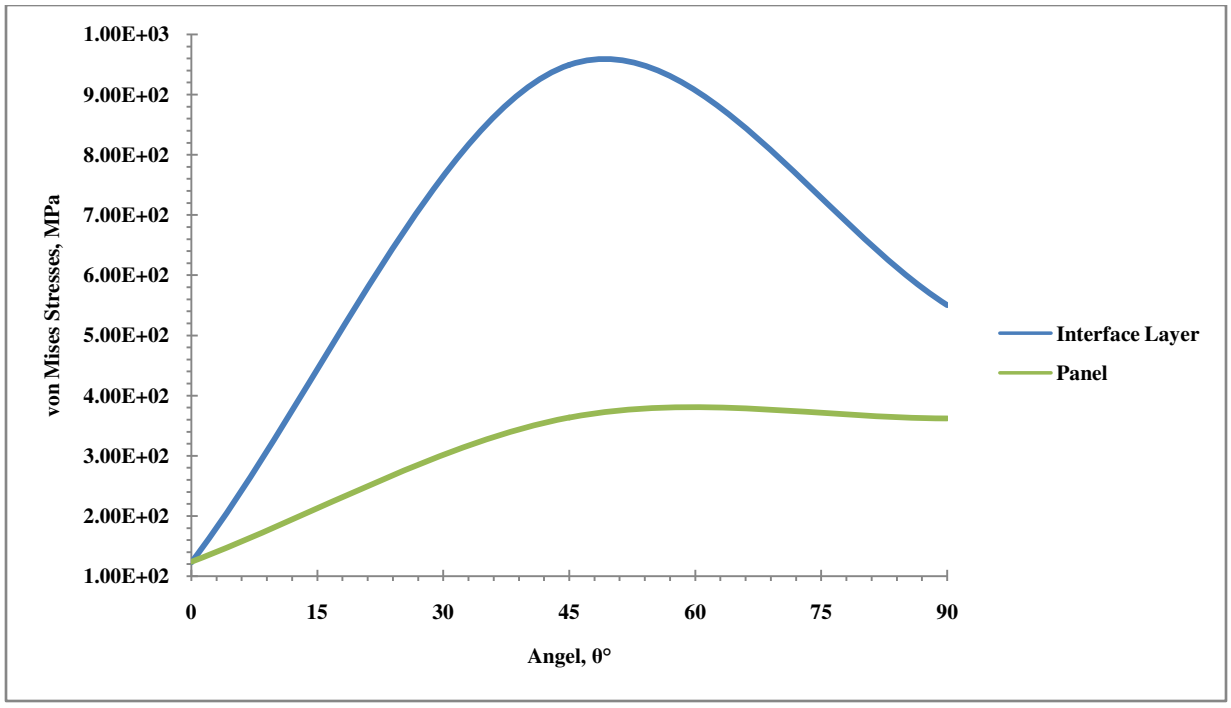

Figure 16: von Mises stress distributions of case 1 on the hull

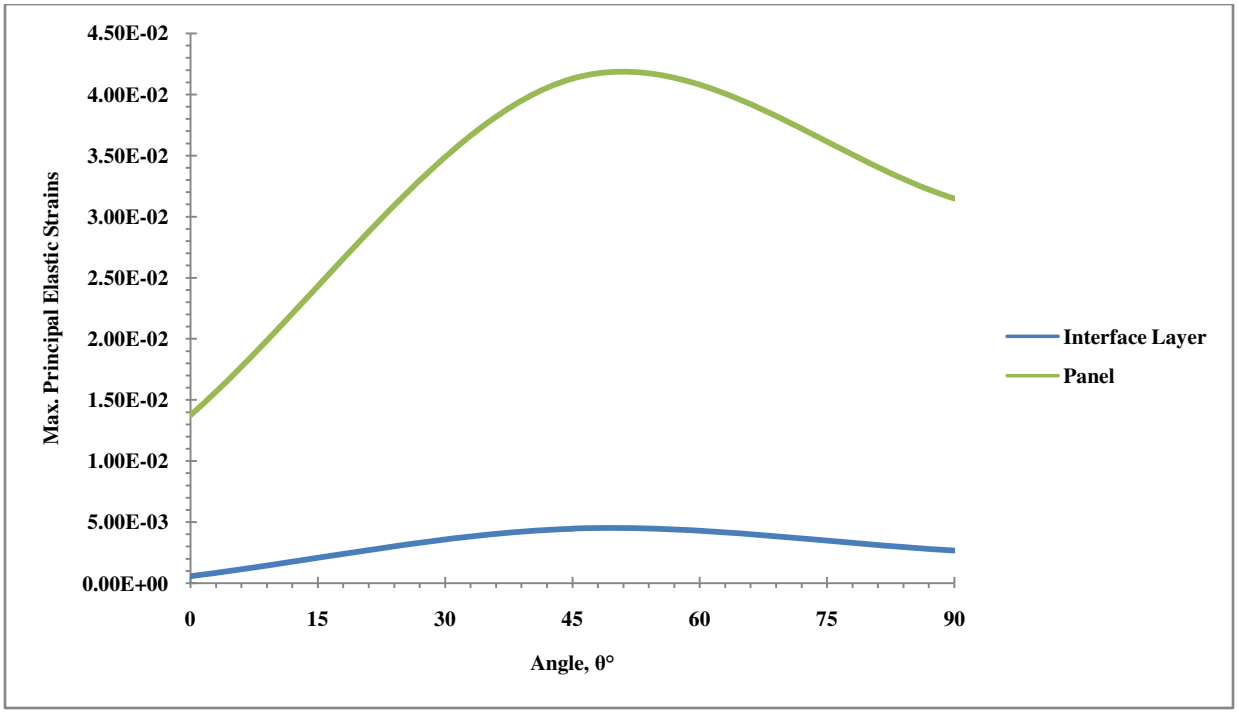

Figure 17: Elastic strain distributions of case 1 on the hull

Similarly, there is an effect of the various patch orientations on each part of the hull structure under the conditions of Case 2, Figures 18 and 19. Increasing the orientation angle of the patch affects the stress and strain distributions on each part of the hull. The reduction in the deformation at the interface layer is significant at 0° with a maximum value of 123 MPa compared with the von Mises stress on the repaired panel. While at 45° and 90°, the reduction of stress levels takes place on the repaired panel.

Table 9: Results and comparisons of stress and strain distributions of the hull model under case 2

Angel, θ	Equivalent Stresses (von Mises, MPa)	
	Interface Layer	Panel
0	1.23E+02	1.25E+02
45	9.85E+02	3.75E+02
90	5.94E+02	3.64E+02
Angel, θ	Maximum Principal Elastic Strains	
	Interface Layer	Panel
0	5.88E-04	1.38E-02
45	4.65E-03	4.60E-02
90	2.87E-03	3.24E-02

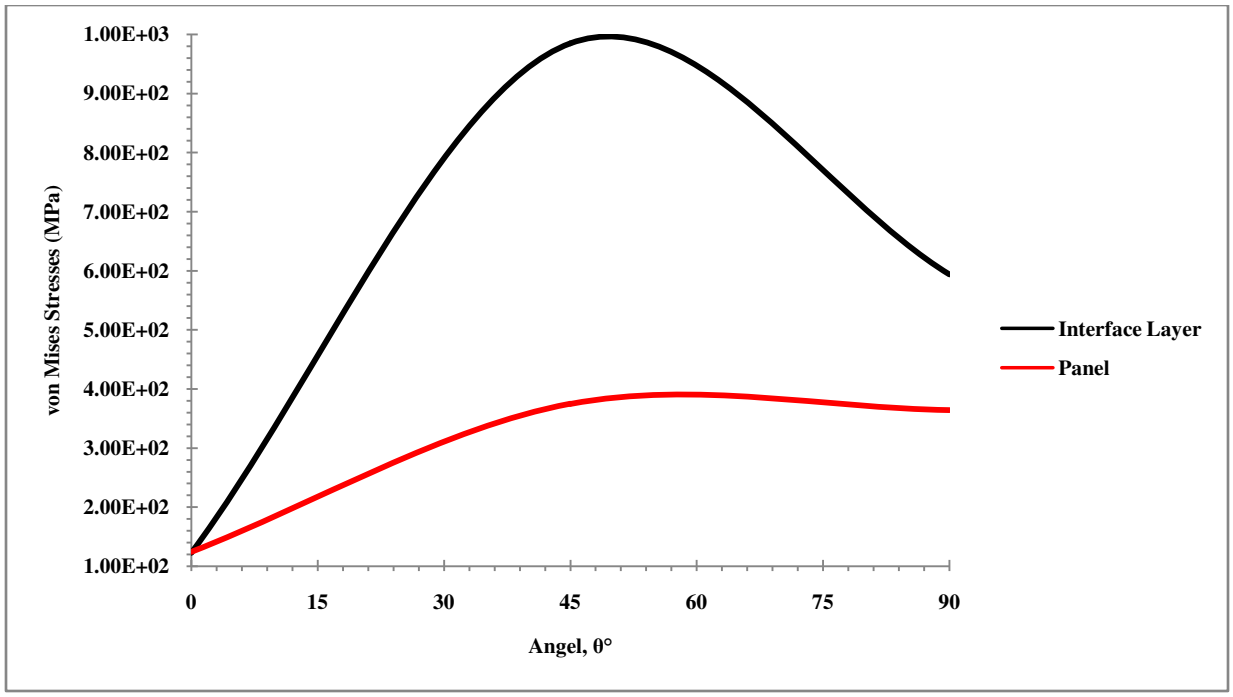

Figure 18: von Mises stress distributions of case 2 on the hull

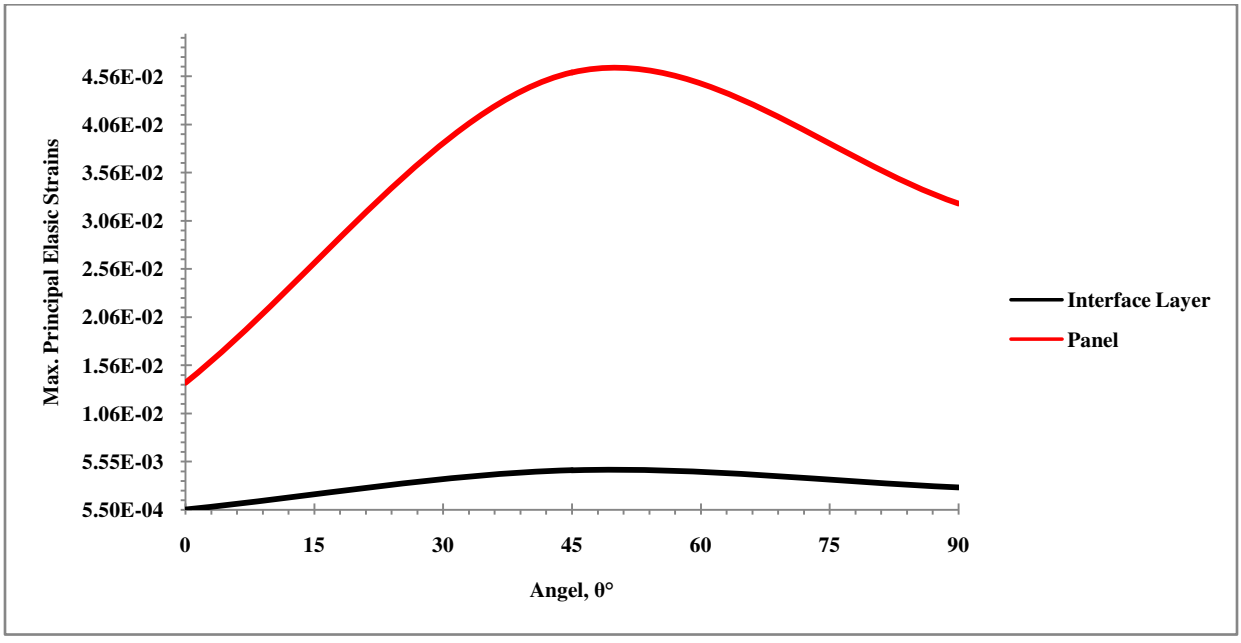

Figure 19: Elastic strain distributions of case 2 on the hull

Stress Concentration Analysis on the Panel

The aim of this present study is additionally to reduce the stress concentrations on the panel. For this reason, another analysis was done to determine the nominal stress, which is needed for the calculation of the stress concentration factor. Stress concentration factor (K_t) is the ratio of the maximum stress (σ_{max}) to the nominal stress (σ_o).

An equivalent 2-D orthotropic panel model has been developed using the same FE code. The geometrical dimensions of the panel are 2800×2400 mm with a thickness of 6 mm, as in Figure 20. The panel has the same equivalent orthotropic properties that were computed early in this chapter. Moreover, the same boundary conditions and loading conditions were applied. From the FE results for the new model and the hull model for case 1, the stress concentration factor at the same applied force of 15 kN is found to be 1.19 for 0° orientation, 3.47 for 45° orientation, and 3.48 for the case of 90° orientations. This interesting result is due to the geometric discontinuities. Calculations of the stress concentration factor are given in Appendix C. These results indicate that with an orientation angle of 0°, there are significant and desirable reductions in stress and strain levels as well as stress concentrations.

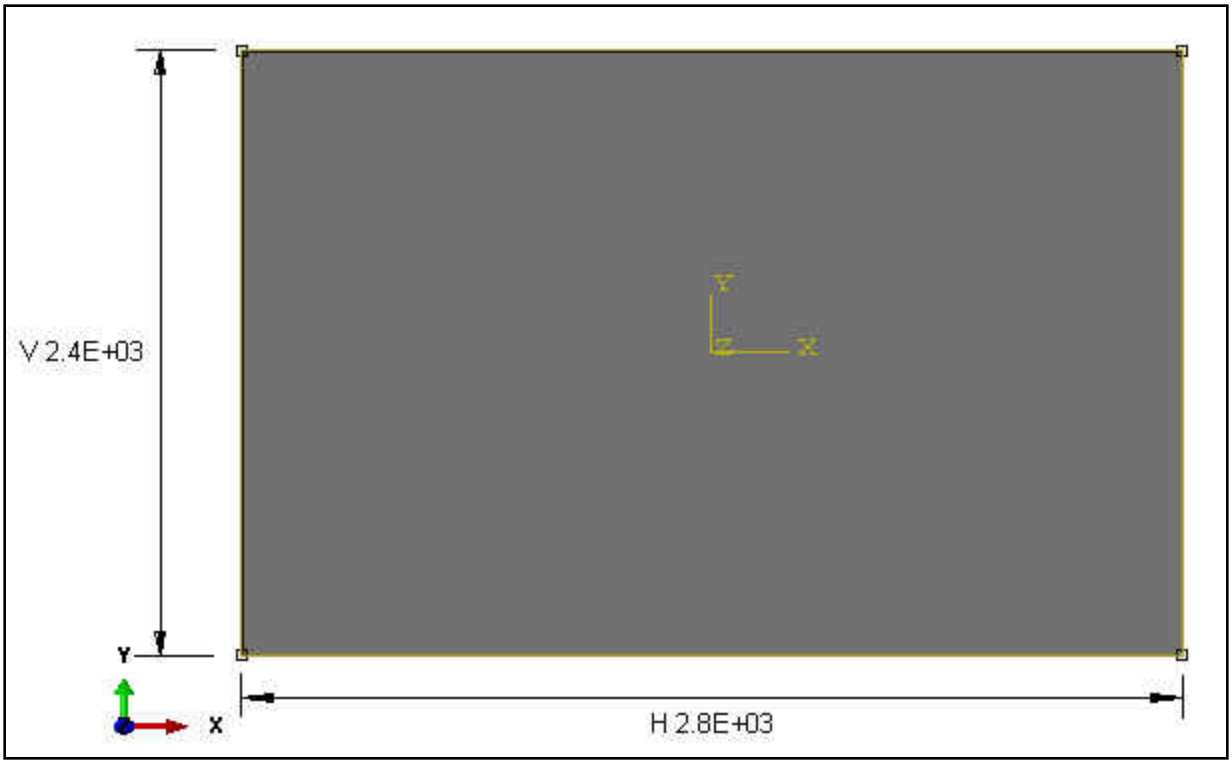

Figure 20: Geometrical dimensions of the panel model

The following figures show the effect of different patch orientations on the isotropic layer. The local FE model is solved in both cases, where the effect of the patch appears to be a sensitive parameter affecting the stress distribution in the structure under the first case of this study.

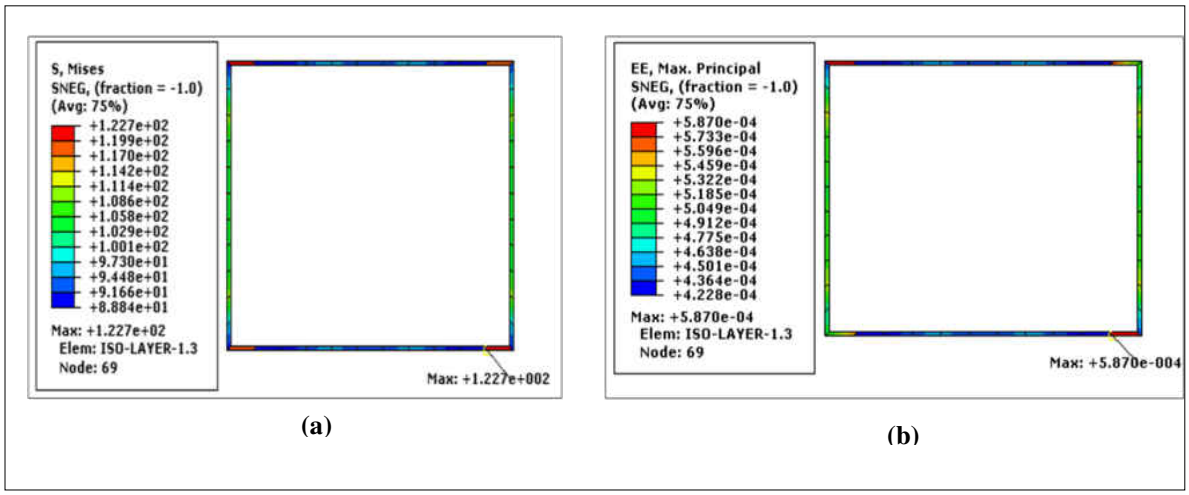

Figure 21: Stress and strain distributions at the interface layer at 0° under case 1 (a) Stress distribution, (b) Strain distribution

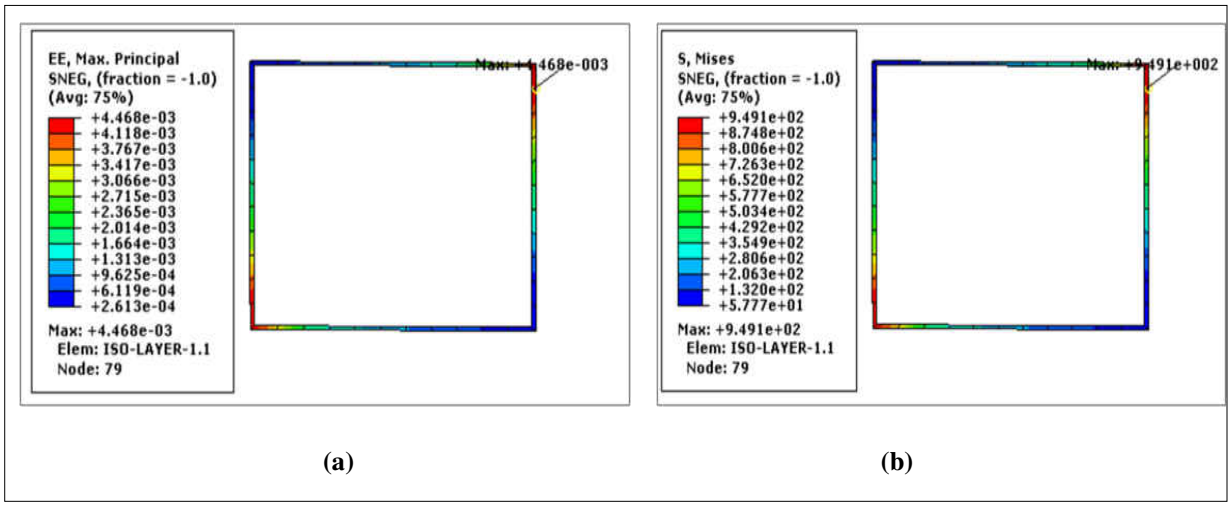

Figure 22: Stress and strain distributions at the interface layer at 45° under case 1 (a) Strain distribution, (b) Stress distribution

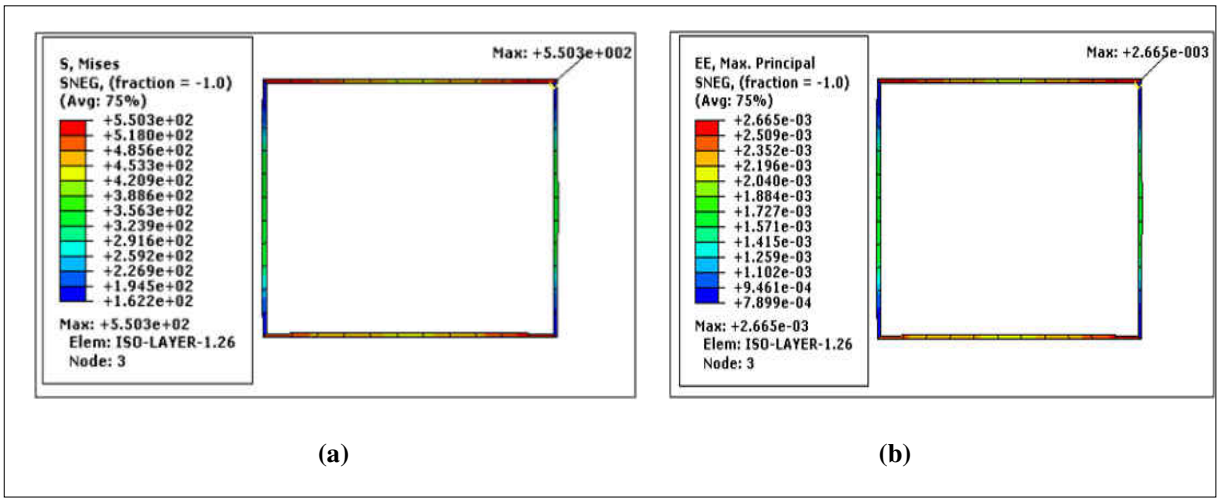

Figure 23: Stress and strain distributions at the interface layer at 90° under case 1 (a) Stress distribution, (b) Strain distribution

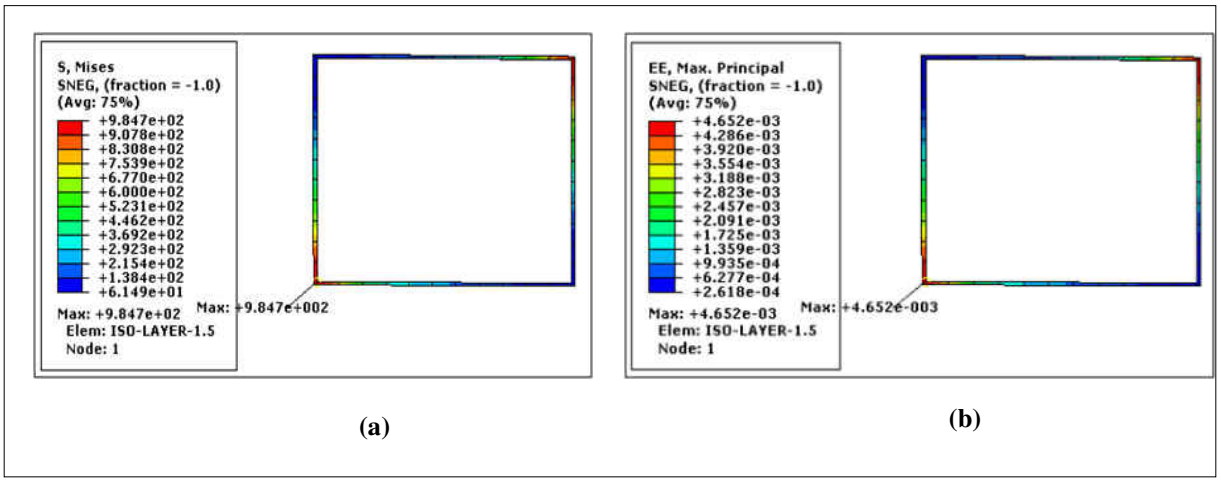

Figure 24: Stress and strain distributions at the interface layer at 0° under case 2 (a) Stress distribution, (b) Strain distribution

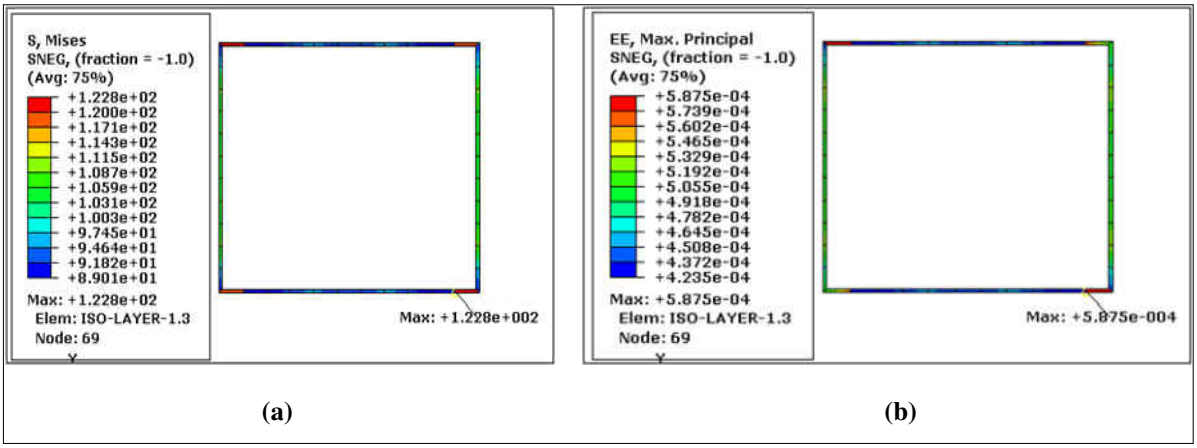

Figure 25: Stress and strain distributions at the interface layer at 45° under case 2 (a) Stress distribution, (b) Strain distribution

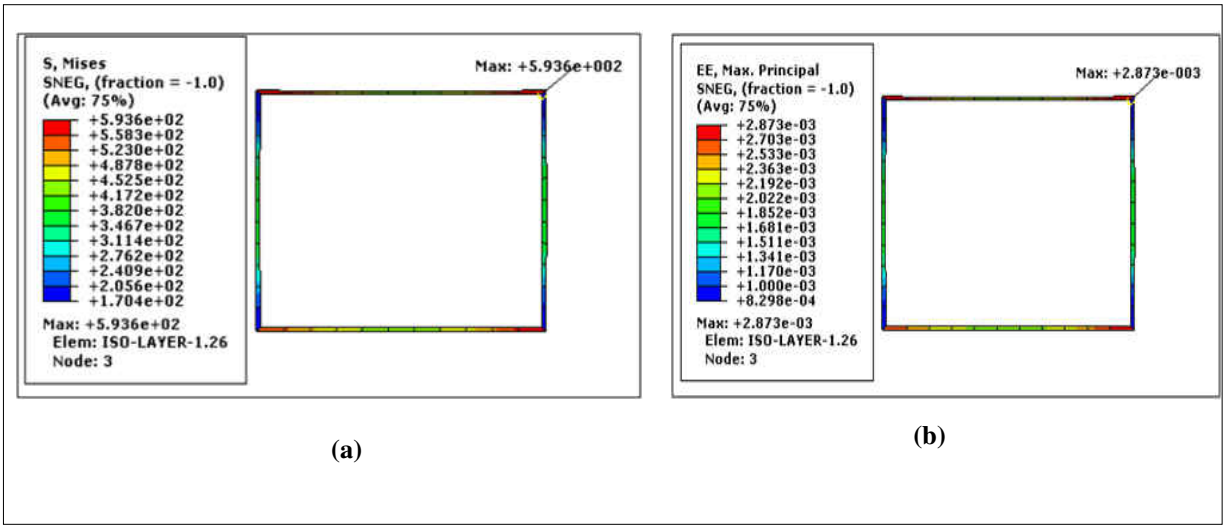

Figure 26: Stress and strain distributions at the interface layer at 90° under case 2 (a) Stress distribution, (b) Strain distribution

The effect of different patch orientations is shown in the following figures. Since the results vary from one angle to another, it is evident that stress and strain reductions take place at the bonded line (isotropic layer) for both cases. At the orientation angle of 0°, the maximum value of the equivalent stress occurred at node 84 on the repaired panel with a value of 124 MPa under Cases 1 and 2, Figures 27 and 30. While at 45°, the stresses in the structure between the patch and the panel which comprise the critical area are extensively higher at nodes 79 and 1 for Case 1 and 2 respectively, Figures 28 and 31 correspondingly. And then the stress concentrations are decreased with the 90° orientation angel at node 3 under both cases. In addition to stress concentrations, strain distributions also vary from one angle to another and from region to region. As seen in Figures 27 (b) through 31 (b), the strain concentrations are critical on the repaired panel for both cases except Case 2 at 90°, in Figure 32 (b), where it is critical on the patch region at node 6.

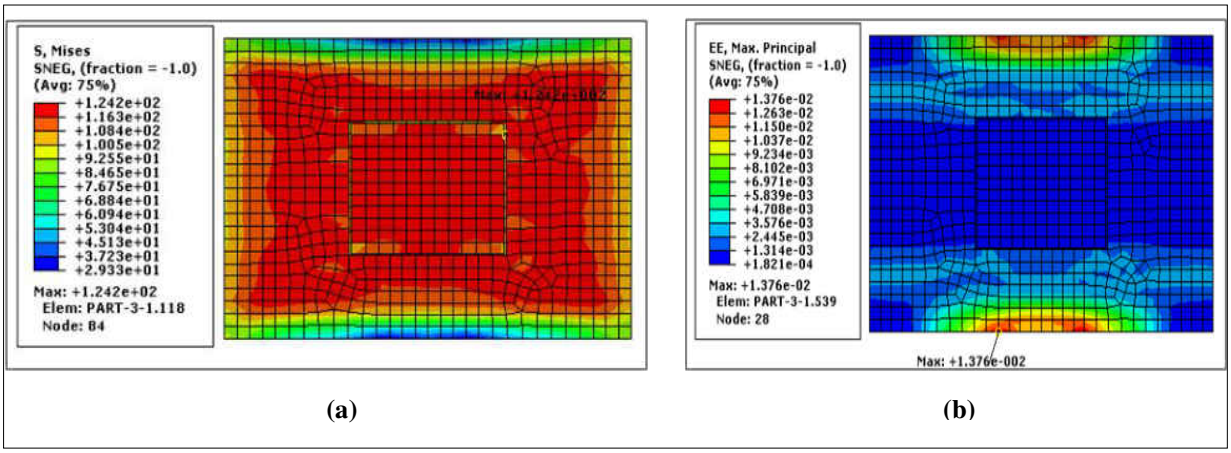

Figure 27: Stress and strain distributions on the hull model at 0° under case 1 (a) Stress distribution, (b) Strain distribution

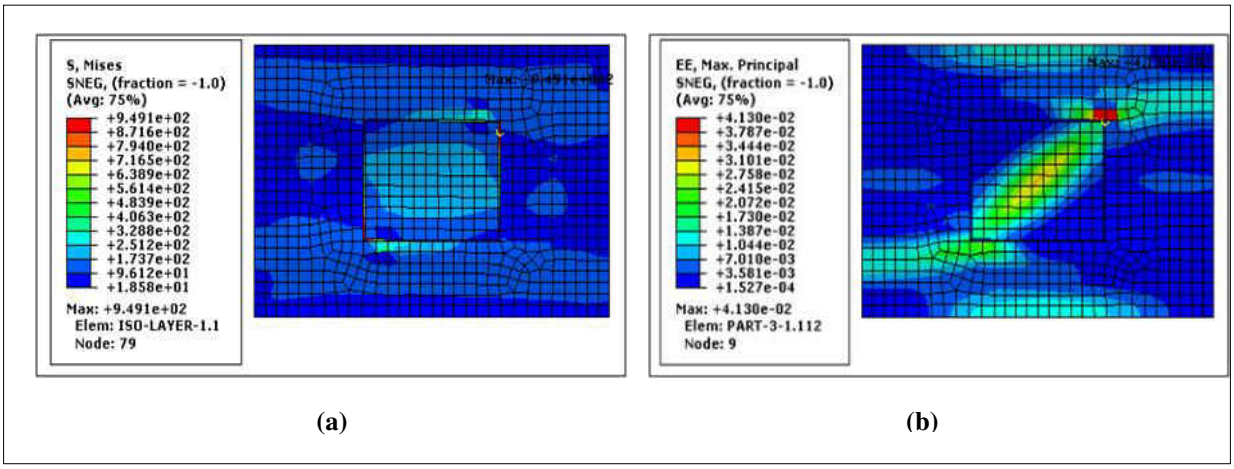

Figure 28: Stress and strain distributions on the hull model at 45° under case 1 (a) Stress distribution, (b) Strain distribution

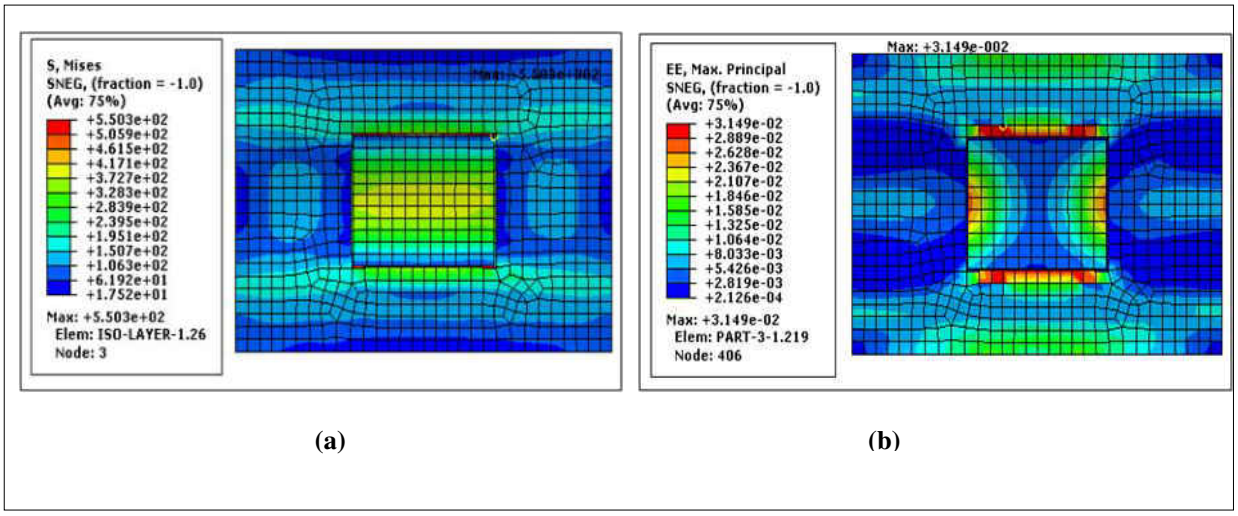

Figure 29: Stress and strain distributions on the hull model at 90° under case 1 (a) Stress distribution, (b) Strain distribution

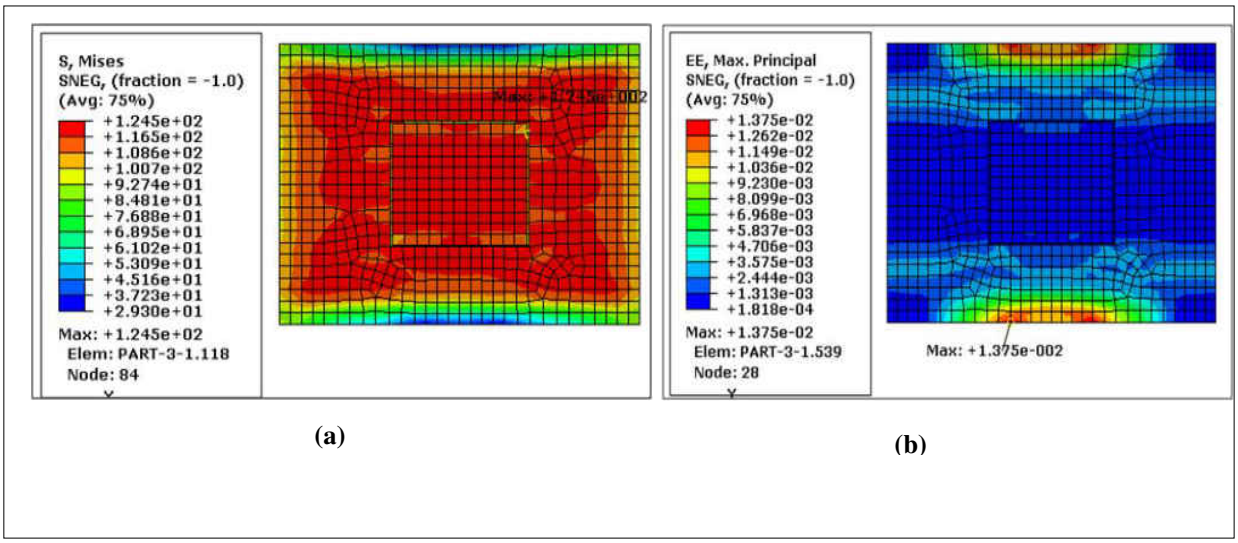

Figure 30: Stress and strain distributions on the hull model at 0° under case2 (a) Stress distribution, (b) Strain distribution

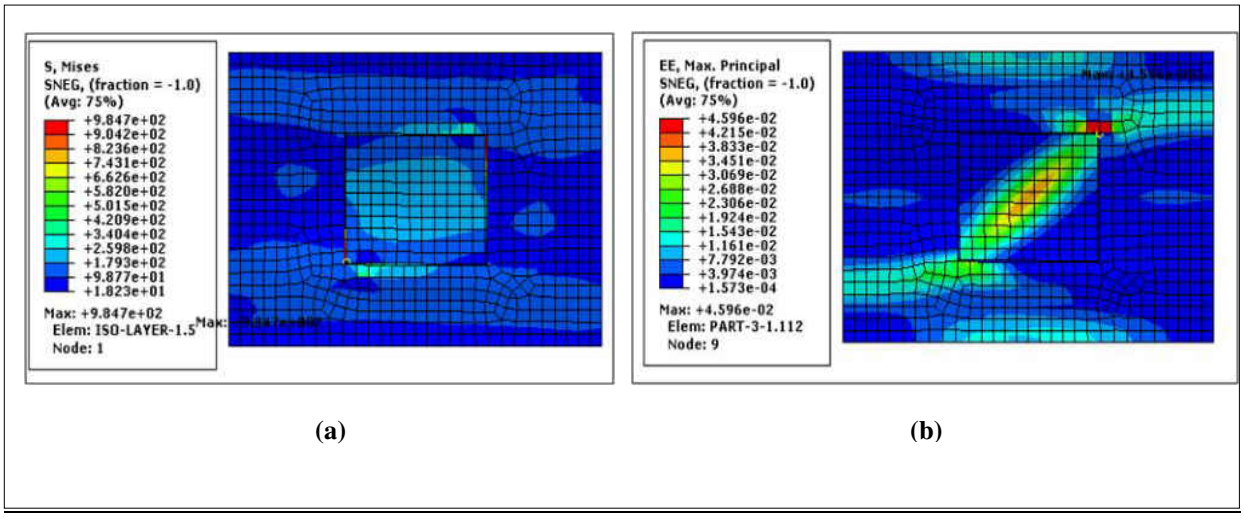

Figure 31: Stress and strain distributions on the hull model at 45° under case 2 (a) Stress distribution, (b) Strain distribution

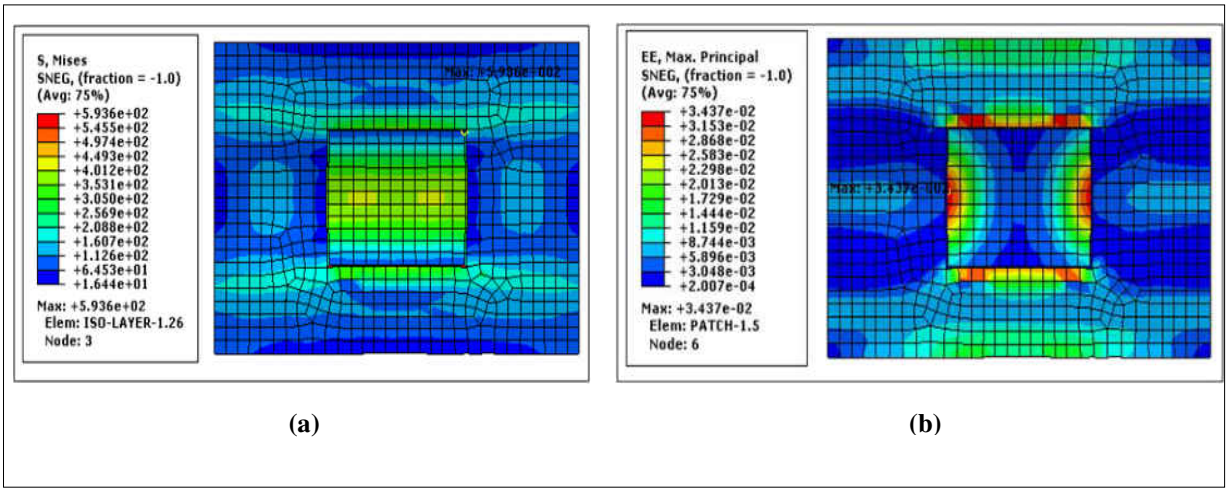

Figure 32: Stress and strain distributions on the hull model at 90° under case 2 (a) Stress distribution, (b) Strain distribution

Discussion of Results

The process of determining the optimal patch orientation for repairing purposes discussed herein shows that the hull is likely capable of sustaining a combination of loading conditions.

A comparison of the ultimate strength results of the hull structure that were obtained from Cases 1 and 2have shown that the stiffer the patch, the lower the level of stress and strain concentration achieved. Comparing the studied cases, the reduction in the stresses and strains, as the material properties of the patch, due to the presence of the orthotropic patch, can be observed. For the second case, this reduction is not much, but as the values of young moduli in the transverse and longitudinal directions increase, the effect of patching increases as well, for the first case.

In addition, the effect of patching material on reducing the strain concentrations at the bond line, as the patch is stiffer, for given geometrical and material parameters, has once again shown that even for a repaired panel, the reduction is likely to happen at 0° with a slight difference between the other two angles, 45° and 90°.

The suggested reason for the difference in reducing the von Mises stresses and strains at the boundaries is due primarily to the effect of the material properties of the equivalent patch, even though the difference of the resulting stresses and strains is insignificant as illustrated for both cases. At 0° orientation, the maximum stress and strain were much lower and displayed much better agreement in reducing the severity of the discontinuity between the panel and patch. The average of the equivalent (von Mises) stress was 122.7 MPa and 587×10^{-6} of the maximum principal strain. This is approximately identical to the result for the same orientation angle of the

other two regions, panel and patch, where the average of the maximum stresses was 124 MPa and 122 MPa respectively.

In both cases, results of various patch orientations of repaired steel panels with 350 mm stiffener spacing and 3 different patch orientation angles of 0°, 45° and 90° indicated that the 0° angle is the best case in reducing the stress and strain concentrations on the hull. However, it should be emphasized that the planes of maximum stresses and strains lie at 45° which indicated that 45° at the bond area is the worst case with an average of 967 MPa, due to the propensity to increase the stress and strain levels.

When the engineering constants of the patch and panel are equal (Case 2), the stress and strain distributions at the interface region when comparing this case with the first case's results, it is evident that the difference in material properties of the panel and patch do not affect the results at 0°. In addition, the stiffer the patch offers higher reduction in the stress and strain levels at rotation angels of 45° and 90°.

Furthermore, results for reducing the stress concentration factors on the panel showed that the 0° case has the lowest stress concentrations. Thus, the reduction is significant when the fiber of the patch aligns with the fiber of the repaired plate.

The finite element results for the studied cases indicate that there is a significant reduction in stress and strain concentrations with 0° orientation. This would benefit the design of the ship hulls and their repairs

The results have proved that the application of orthotropic patch repair successfully reduced the severity of stresses and strains that occur during the repair process of the ship hull.

CHAPTER 5: CONCLUSIONS

From the outset, the goal of this work was to determine the optimal orientation of reduced stress and strain concentrations in maritime vessel hull repair patches using the FEM. For this purpose, an orthotropic plate approach is mainly employed, where elastic constants for orthotropic plates (panels and patches) are determined in a consistent theoretical manner using classical theory of elasticity. The support condition for the panel is assumed to be simply supported along its four edges.

The application of the orthotropic model can be a good replacement to reduce the number of elements needed in the Finite Element model. By reducing the number of elements, computational time can be reduced as well since the number of elements required for the orthotropic model is less than the amount needed for the whole model with corrugation sheets.

The effect of patch fiber with an orientation parallel to the panel fiber directions is more efficient than those with angles almost perpendicular to it. Moreover, it was shown that as the values of engineering constants of the equivalent orthotropic patch increased, the reduction in stresses and strains also increased.

FE modeling showed that the critical stress concentration at the isotropic layer (boundaries) has been reduced, which is demonstrated by the elastic deformation occurring within the boundaries of the composite reinforcement. As expected, the majority of stress and strain reductions occur with 0° orientation.

The use of FE Software ABAQUS and its components tolerate faster and more efficient model generation. The application of varied rotational angles of the equivalent orthotropic patch and the combination of load and boundary conditions are furthermore simpler.

The developed FE model can be used as a fast-evaluated tool to estimate the most efficient orientation and thus, the hull strength after patching process.

Future Work

This study focused only on the determination of various patch orientation and their effect of reducing the stress and strain levels on equivalent orthotropic hull panel. The scope of the current study needs to be expanded to include the effects of other parameters that perform an important role in bringing this study to the reality of implementation. Such parameters can affect the behavior and strength of stiffened panels of a ship's hull. Further studies can be carried out based on the current approach, such as a buckling effect on the repaired hull panel due to different loading conditions, the effect of the number of stiffeners attached to the panel. Simultaneously, the spacing between stiffeners will have an effect on enhancing the result obtained from FE analyses. Also, the effect of patch thickness can be added as well.

In addition, it is important to point out that different geometry of stiffened plates and patches subjected to combined action of in-plane load and lateral pressure can be studied and analyzed. This may be useful for studying and examining different failure modes of ship hull repair. Furthermore, the effect of orthotropic patches and their stiffeners on fatigue crack growth of repaired corrugated steel plates may be considered in this research.

As a step in the direction of developing the repair process of hull structures, a comprehensive Finite Element model has been used. This model has thus far not been verified, yet it is believed to accommodate the main physical effects. Future verification and validation of this FE approach

can be added to this work with experimentation. The experiment can be carried out by using the unit model specimen and full scale specimen to assess the reliability of the repair methodology. However, this will rate the possible usefulness of the numerical approach as a simple and realistic approach for hull strength estimation.

However, for now, if direct study is made with the experimental model, a specimen would be significant in reducing the cost of ship hull repair. New materials and processes can lead to simpler, faster, and cheaper solutions, simplifying maintenance and repair.

Of course, one more extension of this work would be to determine the environmental durability to the development of an adequate design for the use of orthotropic patches in the repair procedure of ship steel structure.

APPENDIX A: DETAILED GEOMETRIES FOR THE SECOND MOMENT OF INERTIA CALCULATIONS

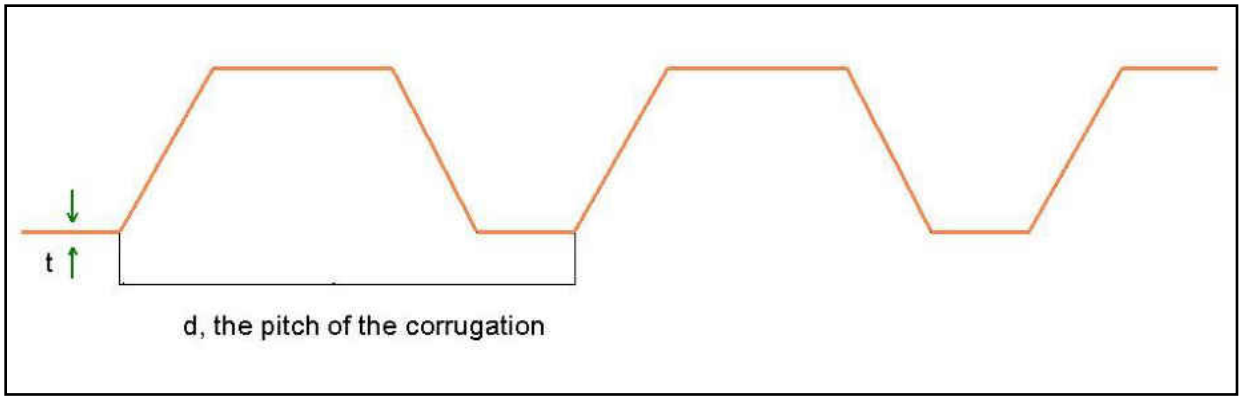

Figure 33: Cross-section of profiled steel sheeting

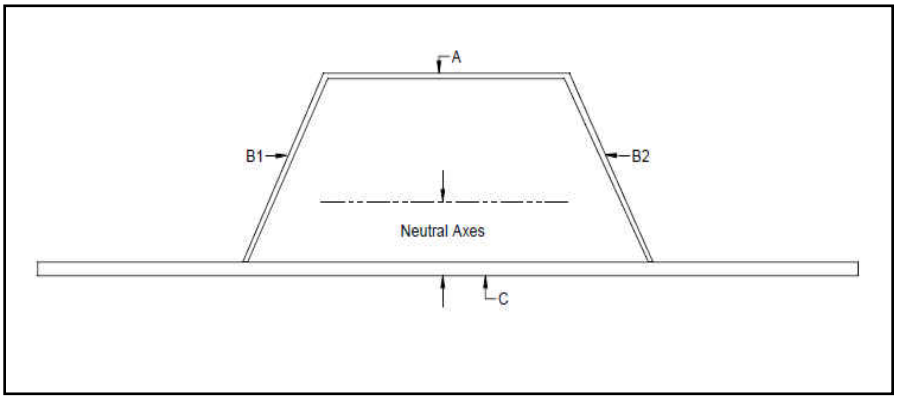

Figure 34: Profiled steel sheeting geometry for stiffened plates

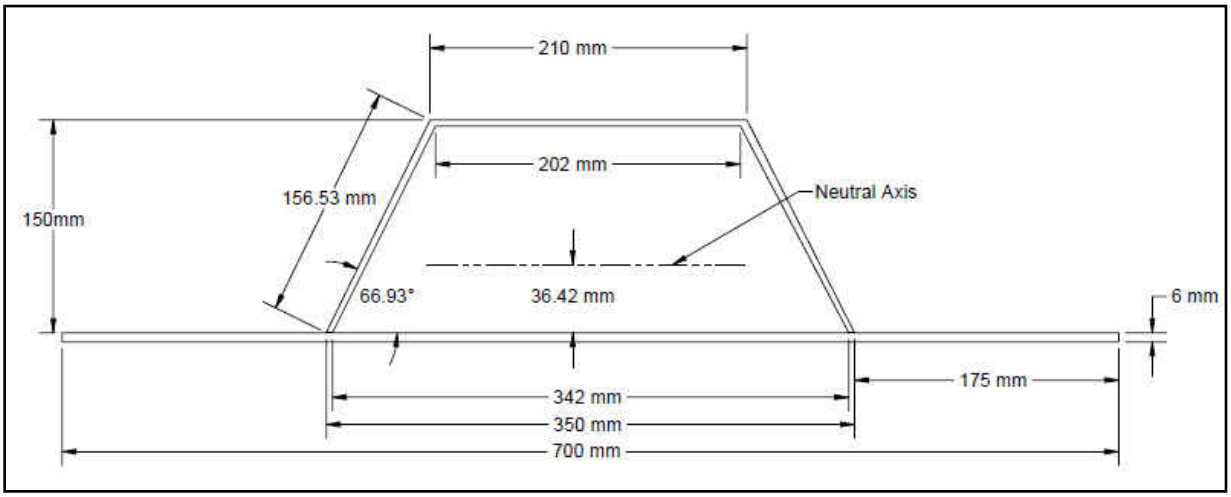

Figure 35: Cross-section of profiled steel sheeting of the panel

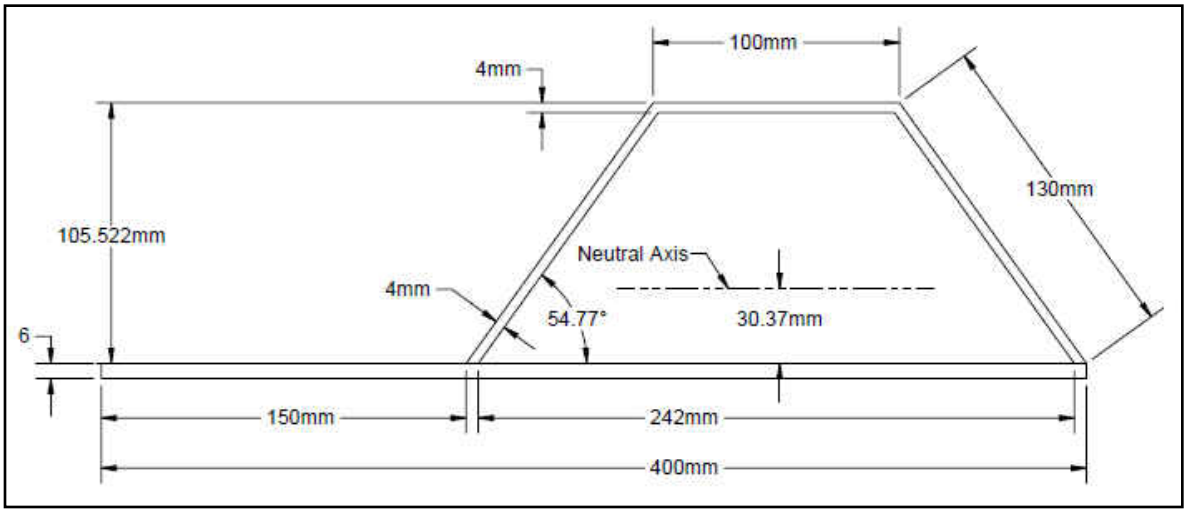

Figure 36: Cross-section of profiled steel sheeting of the patch

APPENDIX B: DETAILED GEOMETRIES FOR DETERMINING THE $\bar{K}$ VALUES FOR FASTENERS IN EVERY THROUGH

The value for the dimensionless constant $\overline{K}$ for sheet distortion depends on many factors. These parameters are described as following;

- The ratio between the profile dimensions and the pitch of corrugations ($\frac{2b_T}{d}$),
- The angle Theta (θ), and
- The ratio between the height of sheeting profile and the pitch of corrugations, (h/d).

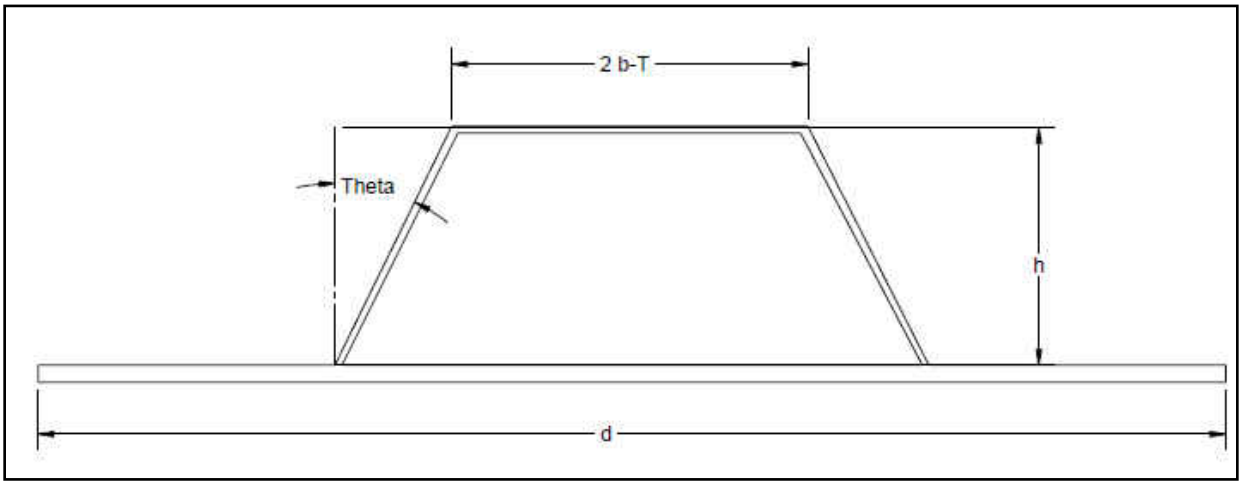

Figure 37: Determination of $\overline{K}$ value for fasteners in every through

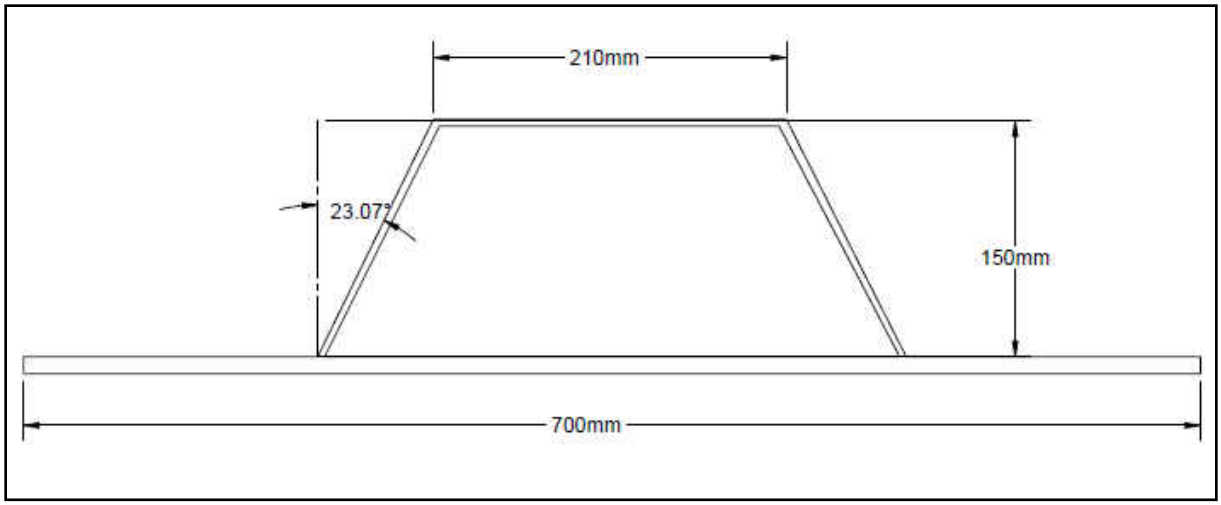

Figure 38: Determination of $\bar{K}$ value for panel fasteners in every through

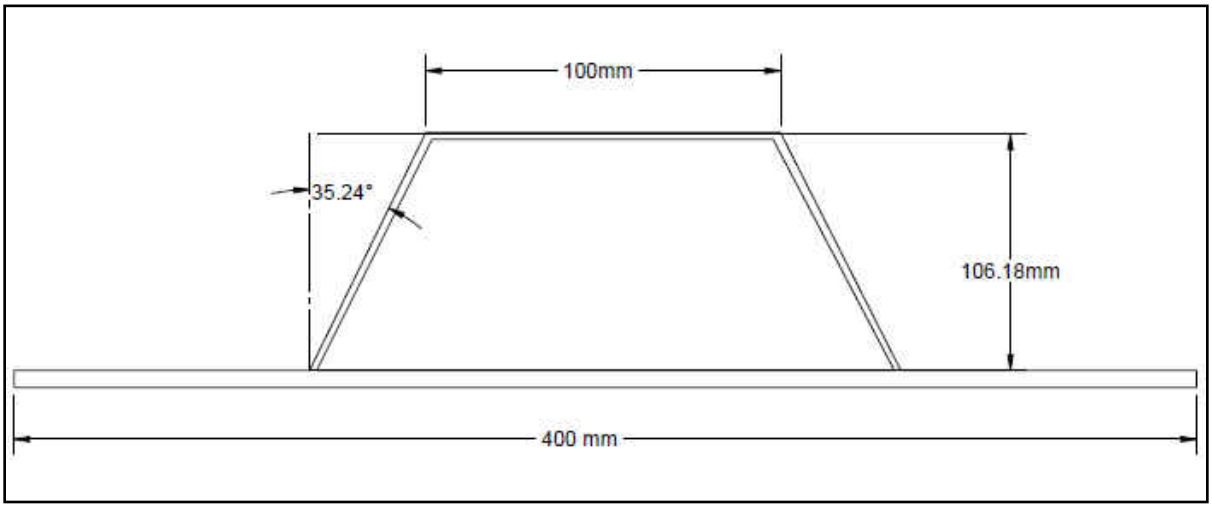

Figure 39: Determination of $\bar{K}$ value for patch fasteners in every through

APPENDIX C: CALCULATIONS OF STRESS CONCENTRATION FACTOR (K_t)

A stress concentration factor is known as the ratio of the maximum stress and nominal stress. The following procedure is followed to calculate K_t for different orientation angles.

$$K_t = \frac{\sigma_{max}}{\sigma_{nom}} \tag{10}$$

From Table 8, the maximum von Mises stresses on the panel at equivalent force loading of 15 kN are; 124 MPa at 0°, 364 MPa at 45°, and 362 at 90°. And from Figure 39, the nominal stress at the same force loading is 104.5 MPa. The value of nominal stress was picked base on the homogeneity of stress distribution on the panel. In other words, the middle area of the panel has a constant distribution of stresses with an approximate value of 104.5 MPa. Hence;

From Equation 10, and for 0° orientation,

$$K_t = \frac{124}{104.5} = 1.19$$

For 45° orientation,

$$K_t = \frac{364}{104.5} = 3.48$$

Finally, for 90° orientation,

$$K_t = \frac{362}{104.5} = 3.47$$

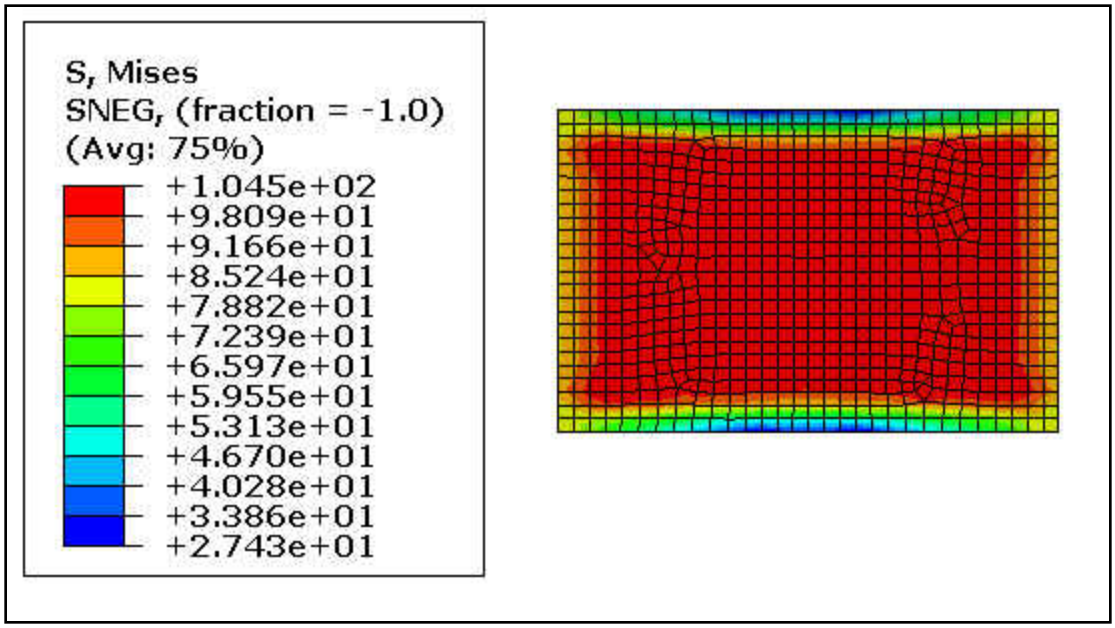

Figure 40: Stress concentration on the panel

LIST OF REFERENCES

[1] Abaqus. (2011). Analysis User's Manual *Volume IV: Elements*. USA: Dassault Systèmes.

[2] ABS, American Bureau of Shipping Incorporated;. (2007). SHIPBUILDING AND REPAIR QUALITY STANDARD FOR HULL STRUCTURES DURING CONSTRUCTION.

[3] Ahmed, E, & Wan Badaruzzaman, W. H. (2003). Equivalent Elastic Analysis of Profiled Metal Decking Using Finite Element Method. *Steel Structures, 3*, 9-17.

[4] Amdahl, Jorgen (2008). TMR4205 Buckling and Ultimate Strength Analysis of Marine Structures. *Institutt for marin teknikk*. <http://www.ivt.ntnu.no/imt/courses/tmr4205/literature/chpt3.buckling of stiffened plates-mai2009.pdf>.

[5] ASCHEMEIER, UWE. (2013). Repair of a Hull 15 m below the Waterline. In F. D. t. t. hull & v. f. t. outside. (Eds.): Welding Jouranal.

[6] Assakkaf, Ibrahim A, Ayyub, Bilal M, Hess, Paul E, & Atua, Khaled (2008). Reliability-Based Loads and Resistance Factor (LFRD) Guidlines for Stiffened Panels and Grillages of Ship Structures. *114*, 89-112. doi: 10.1111/j.1559-3584.2002.tb00126.x

[7] BEBON, Henan (2011). AH36 Shipbuilding steel plate. from http://www.shipbuilding-steel.com/Products/AH36.html

[8] Byklum, Eirik, Steen, Eivind , & Amdahl, Jørgen (2004). A semi-analytical model for global buckling and postbuckling analysis of stiffened panels. *Thin-Walled Structures, 42*(2004), 701-717.

[9] Chen, Nina-zhong, Sun, Hail-Hong , & Soares, Guedes C. . (2003). Reliability Analysis of a Ship Hull in Composite Materials. *Composite Structures, 62*(2003), 59-66.

[10] Cullen, Lauren E. (2007). *An Evaluation of the Strength Characteristics of Horizontally Curved Steel I-Girder Bridges.* (Master of Science), West Virginia University, Mogantown, WV. (1451625)

[11] Davies, J. M, & Lawson, R. M. (1978). The shear deformation of profiled metal sheeting. *International Journal for numerical moethods in engineering, 12*(10), 1507-1541.

[12] Demibilek, Zeki. (1989). *Tension Leg Platform*: The American Society of Civil Engineers.

[13] DNV-Standard. (2012). Design, Fabrication, Operation and Qualification of Bonded Repair of Steel Structures (Vol. DNV-RP-C301, pp. 62). DET NORSKE VERITAS AS.

[14] Grabovac, Ivan , & Whittaker, David (2009). Application of bonded composites in the repair of ships structures – A 15-year service experience. *Composites: Part A, 40*(2009), 1381–1398.

[15] Greene, Eric (1999). *Marine Composites*. Annapolis, Maryland 21403: Eric Greene Associates, Inc.

[16] Halliwell, Sue. (2007). Repair of Fiber Reinforcement Polymer Structures. *National Composites Network*.

[17] Hosseini-Toudeshky, H, Ghaffari, M. Ali , & Mohammadi, Bijan (2012). Finite element fatigue propagation of induced cracks by stiffeners in repaired panels with composite patches. *Composite Structures, 94*(5), 1771-1780.

[18] Ma, Sinyuan , & Mahfuz, Hassan (2012). Finite Element Simulation of Composite Ship Structures with Fluid Structure Interacction. *Ocean Engineering, 52*(2012), 52-59.

[19] Military. (2013). The Hull *http://www.globalsecurity.org/military/systems/ship/hull.htm*.

[20] Milligan, Dan. (2012). Converging on Composites. Retrieved from http://info.firehole.com/blog/?Tag=reaction%20forces

[21] Munters. Ship Hull Repair.

[22] Okafor, A. C, S, N, Enemuoh, U.E, & Rao, S.V. (2005). Design, analysis and performance of adhesively bonded composite patch repair of cracked aluminum aircraft panels. *Composite Structures, 71*(2), 258-270.

[23] Okumoto, Y, Takeda, Y, Mano, M, & Okada, T. (2009). *Design of Ship Hull Structures A Practical Guide for Engineers*. Verlag Berlin Heidelberg: Springer.

[24] PG, SUNIL KUMAR (2008). *FINITE ELEMENT ANALYSIS OF WARSHIP STRUCTURES.* (DOCTOR OF PHILOSOPHY), COCHIN UNIVERSITY OF SCIENCE AND TECHNOLOGY, KOCHI - 682 022, KERALA. (2748)

[25] Soares, C. Guedes , & Garbatov, Y. (1996). Fatigue reliability of the ship hull girder accounting for inspection and repair. *Reliability Engineering and System Safety, 51*(1996), 341-335 I.

[26] Steen, Eivind (2013). Ship Hull Strength-what Are the Limits and How to Assess Them? *Explaning Non-Linear FE Analysis*. <http://www.dnvusa.com/industry/maritime/publicationsanddownloads/pu>

[27] Sunyong Kim, D. M. F. (2010). Optimum inspection planning for minimizing fatigue damage detection delayof ship hull structures. *International Journal of Fatigue, 33*(2011), 448-459.

[28] Tharian, Manoj G , & G, nandakumar C (2013). Hat Stiffened Plates for Ship Building. *International Journal of Applied Engineering, 3*(1), 1-10.

[29] Ting, T, Jones, R, Chiu, W.K, Marshall, I.H , & Greer, J.M. (1999). Composite repairs to rib stiffened panels. *Composite Structures, 47*(1999), 737-743.

[30] Walsh, J. , Hou, G. , & Soman, K. . (2008). *A Comparison of Slamming Impact Models on Orthotropic Sandwich Panels*. Paper presented at the International conference on high performance structures and materials

4th, International conference on high performance structures and materials.

[31] Wennberg, David, Wennhage, Per , & Stichel, Sebastian (2011). Orthotropic Models of Corrugated Sheets in Finite Element Analysis.

[32] Zachariah, K. Z, Iyer, Nagesh R, & Rao, T. Appa (1989). Modelling of Ship Hull Structures for Finite Element Analysis. *Engineering Software*, 757-768.

[33] Zhang, Wei , Cai, C.S, & Pan, Fang (2013). Finite Element Modeling of Bridges with Equivalent Orthotropic Material Methodfor Multi-Scale Dynamic Loads. *Engineering Structures, 54*, 82-93.

[34] Ziha, K, Goles, S, Radica, A, & Maskimovic, S. (2005). Effects of Hull Deformations on Ship Displacement. *Maritime Transportation and Exploitation of Ocean and Coastal Resources; Proceedings of the 12th International Congress of the International Maritime*, 599-605.